Baryogenesis in a parity solution to the strong CP problem

Keisuke Harigaya[a,b,c,d] **and Isaac R. Wang**[e]

[a]*Department of Physics, University of Chicago,*
Chicago, IL 60637, U.S.A.

[b]*Enrico Fermi Institute and Kavli Institute for Cosmological Physics, University of Chicago,*
Chicago, IL 60637, U.S.A.

[c]*Kavli Institute for the Physics and Mathematics of the Universe (WPI),*
The University of Tokyo Institutes for Advanced Study, The University of Tokyo,
Kashiwa, Chiba 277-8583, Japan

[d]*Theoretical Physics Department, CERN,*
1211 Geneva 23, Switzerland

[e]*New High Energy Theory Center, Department of Physics and Astronomy, Rutgers University,*
Piscataway, NJ 08854, U.S.A.

E-mail: kharigaya@uchicago.edu, isaac.wang@rutgers.edu

ABSTRACT: Space-time parity can solve the strong CP problem and introduces a spontaneously broken $SU(2)_R$ gauge symmetry. We investigate the possibility of baryogenesis from a first-order $SU(2)_R$ phase transition similar to electroweak baryogenesis. We consider a model with the minimal Higgs content, for which the strong CP problem is indeed solved without introducing extra symmetry beyond parity. Although the parity symmetry seems to forbid the $SU(2)_R$ anomaly of the $B - L$ symmetry, the structure of the fermion masses can allow for the $SU(2)_R$ sphaleron process to produce non-zero $B - L$ asymmetry of Standard Model particles so that the wash out by the $SU(2)_L$ sphaleron process is avoided. The setup predicts a new hyper-charged fermion whose mass is correlated with the $SU(2)_R$ symmetry breaking scale and hence with the $SU(2)_R$ gauge boson mass, and depending on the origin of CP violation, with an electron electric dipole moment. In a setup where CP violation and the first-order phase transition are assisted by a singlet scalar field, the singlet can be searched for at future colliders.

Contents

1 Introduction

The CP phases in the quark masses, which explain the CP violation in the weak interaction, are expected to also introduce CP violation in the strong interaction [1–4]. However, the CP-violating phase in the strong interaction is known to be smaller than 10^{-10} from the

non-observation of the neutron electric dipole moment (EDM) [5]. This discrepancy is called the strong CP problem.

The absence of the strong CP violation can be explained by a space-time parity symmetry [6, 7], which predicts the parity partner of the $SU(2)_L$ gauge symmetry called the $SU(2)_R$ gauge symmetry. The $SU(2)_R$ gauge symmetry must be spontaneously broken at an energy scale higher than the electroweak scale to explain the absence of $SU(2)_R$ gauge bosons at the electroweak scale.

A model with an $SU(2)_L$-doublet Higgs H_L and an $SU(2)_R$-doublet Higgs H_R is particularly appealing since the Higgs potential does not contain any physical phases and the strong CP problem is indeed solved without introducing extra symmetries [8, 9]; see [6, 7, 10, 11] for setups with a different Higgs content and additional symmetries. Quantum corrections to the strong CP phase are computed in [12, 13] and are found to be sufficiently small.

In this paper, we pursue a possible cosmological role of the $SU(2)_R$ gauge symmetry; production of the baryon asymmetry of the universe. The baryon symmetry has $SU(2)_R$ anomaly and is violated by $SU(2)_R$ sphaleron processes. As in electroweak baryogenesis [14], the baryon asymmetry of the universe may be produced from this baryon number violation, a first-order $SU(2)_R$ phase transition, and some CP violation in the early universe.

There seems to be an apparent obstacle to this idea. The Standard model (SM) $B - L$ symmetry does not have $SU(2)_L$ anomaly, so the parity symmetry seems to require that $B - L$ symmetry also does not have $SU(2)_R$ anomaly. The first-order $SU(2)_R$ phase transition cannot create $B - L$ asymmetry, and baryon asymmetry produced by the $SU(2)_R$ phase transition will be immediately washed out by the $SU(2)_L$ sphaleron process. This naive expectation assumes that the asymmetry of $SU(2)_R$ charged particles is rapidly transferred into that of $SU(2)_L$ charged particles. This is indeed the case in the models where the SM Higgs and right-handed fermions are embedded into a bi-fundamental Higgs Φ and $SU(2)_R$ doublet fermions $\bar{f}$ respectively, and the SM Yukawa couplings come from $f\Phi\bar{f}$, where f are SM $SU(2)_L$-doublet fermions. As we will see, this is not necessarily the case in the model with H_L and H_R, and the washout may be avoided.

Our scenario predicts a hyper-charged fermion with a mass given by $m_i v_R/v_L$, where i is e, μ, or τ, and v_R and v_L are $SU(2)_R$ and $SU(2)_L$ symmetry breaking scale, respectively. The mass of the new fermion is then correlated with the masses of $SU(2)_R$ gauge bosons, and with the electron EDM, depending on the source of CP violation. The case with $i = \tau$ is particularly interesting since v_R predicted from the allowed range of the new fermion mass ($\gtrsim 100\,\text{GeV}$) overlaps with v_R that is accessible at near future colliders and measurements of the electron EDM.

The first-order $SU(2)_R$ phase transition may be achieved as in electroweak baryogenesis, namely, by a thermal potential from a quartic coupling [15–23] or an (effective) tree-level trilinear coupling [24–29] of H_R with a new scalar. We consider two examples without hierarchy problems beyond that of H_L and H_R. We analyze a model with singlet scalar fields with the minimal coupling to H_L and H_R that was analyzed for electroweak baryogenesis [30, 31]. We may also utilize the running of the Higgs quartic coupling; the quartic coupling of H_L becomes small at high energy scales, so if v_R is sufficiently high, the

quartic coupling of H_R, which is equal to that of H_L evaluated at v_R, can be small enough for a first-order $SU(2)_R$ phase transition to occur. If the running is induced only by the SM interaction, v_R is required to be above 10^8 GeV, but extra interactions of H_L can lower v_R.

CP violation can be obtained in various ways. Note that the parity symmetry does not forbid the CP phases of the theory; it only puts relations among them. As an example, we consider CP violation from a dimension-6 coupling between H_R and the $SU(2)_R$ gauge bosons [32] and that from a dimension-5 coupling between a singlet scalar and the $SU(2)_R$ gauge bosons. Those couplings induce non-zero EDMs of SM fermions. That of an electron is detectable by near future experiments if $v_R = O(10)$ TeV, for which the new hyper-charged fermion is within the reach of near-future colliders.

There are several past works on first-order $SU(2)_R$ phase transitions. Ref. [33] investigated $SU(2)_R$ breaking by a triplet scalar and computed the resultant gravitational-wave spectrum. Ref. [34] considers a model of baryogenesis with extra chiral $SU(2)_R$ charged fermions and the possible embedding of the model into a parity-symmetric theory by further extending the gauge group at UV. See [35–39] for baryogenesis models from a new non-Abelian gauge symmetry other than $SU(2)_R$.

This paper is organized as follows. In section 2, we describe a parity-symmetric model with H_L and H_R. We discuss how the fermion masses, including the neutrino masses, are obtained. In section 3, we present a model of baryogenesis from the $SU(2)_R$ phase transition. Experimental signals are discussed in section 4. Finally, a summary and discussion are given in section 5.

2 A parity-symmetric model

In this section, we describe a parity-symmetric model we study.

2.1 Gauge symmetry breaking

The gauge symmetry at UV is $SU(3)_c \times SU(2)_L \times SU(2)_R \times U(1)_X$, which is broken down to the SM gauge symmetry by the vacuum expectation value (VEV) of $H_R(\mathbf{1}, \mathbf{1}, \mathbf{2}, 1/2)$. The SM gauge symmetry is broken down to $SU(3)_c \times U(1)_{\mathrm{EM}}$ by the VEV of $H_L(\mathbf{1}, \mathbf{2}, \mathbf{1}, -1/2)$.

We impose a parity symmetry $H_R \leftrightarrow H_L^\dagger$ that solves the strong CP problem [8, 9] as we will see. The parity-symmetric potential of H_L and H_R is

$$V = \lambda \left(|H_R|^4 + |H_L|^4 \right) + \lambda_{LR}|H_L|^2|H_R|^2 - m^2 \left(|H_R|^2 + |H_L|^2 \right). \tag{2.1}$$

The mass of the $SU(2)_R$ gauge boson must be much larger than that of the electroweak gauge boson. At the tree level, however, there is no vacuum with $v_R > v_L \neq 0$ for any choice of the parameters of potential. Such a phenomenologically viable vacuum can be obtained by softly breaking the parity symmetry [8, 9],

$$\Delta V = -\Delta m^2 \left(|H_R|^2 - |H_L|^2 \right), \quad \Delta m^2 > 0, \tag{2.2}$$

or by quantum corrections to the Higgs potential [12]. In this paper, we consider the former option, since the latter option leads to the production of domain walls upon $SU(2)_R$ phase transition. The soft breaking may be understood as spontaneous breaking by a field that couples to H_L and H_R.

	H_L	H_R	q_i	$\bar{q}_i$	ℓ_i	$\bar{\ell}_i$	U_i	$\bar{U}_i$	D_i	$\bar{D}_i$	E_i	$\bar{E}_i$
$SU(3)_c$	$\mathbf{1}$	$\mathbf{1}$	$\mathbf{3}$	$\bar{\mathbf{3}}$	$\mathbf{1}$	$\mathbf{1}$	$\mathbf{3}$	$\bar{\mathbf{3}}$	$\mathbf{3}$	$\bar{\mathbf{3}}$	$\mathbf{1}$	$\mathbf{1}$
$SU(2)_L$	$\mathbf{2}$	$\mathbf{1}$	$\mathbf{2}$	$\mathbf{1}$	$\mathbf{2}$	$\mathbf{1}$	$\mathbf{1}$	$\mathbf{1}$	$\mathbf{1}$	$\mathbf{1}$	$\mathbf{1}$	$\mathbf{1}$
$SU(2)_R$	$\mathbf{1}$	$\mathbf{2}$	$\mathbf{1}$	$\mathbf{2}$	$\mathbf{1}$	$\mathbf{2}$	$\mathbf{1}$	$\mathbf{1}$	$\mathbf{1}$	$\mathbf{1}$	$\mathbf{1}$	$\mathbf{1}$
$U(1)_X$	$-\frac{1}{2}$	$\frac{1}{2}$	$\frac{1}{6}$	$-\frac{1}{6}$	$-\frac{1}{2}$	$\frac{1}{2}$	$\frac{2}{3}$	$-\frac{2}{3}$	$-\frac{1}{3}$	$\frac{1}{3}$	-1	1

Table 1. The gauge charges of Higgses and fermions.

This theory in general has three tuning; small $m^2/\Lambda_{\rm UV}^2 \sim v_R^2/\Lambda_{\rm UV}^2$, small $\Delta m^2/\Lambda_{\rm UV}^2 \sim v_R^2/\Lambda_{\rm UV}^2$, and small $(m^2 - \Delta m^2)/m^2 \sim v_L^2/v_R^2$, where $\Lambda_{\rm UV}$ is the UV scale. One may remove the second one by generating Δm^2 by dynamical transmutation. The total fine-tuning is $v_R^2/\Lambda_{\rm UV}^2 \times v_L^2/v_R^2 = v_L^2/\Lambda_{\rm UV}^2$ and is the same as the SM. This tuning may be explained by anthropic principle [40–42]. One can also remove the first tuning by embedding the theory into solutions to the EW hierarchy problems with a mass scale $\sim v_R^2$, such as supersymmetric or composite scenarios. The last tuning v_L^2/v_R^2, however, cannot be removed.

2.2 Charged fermion masses

The quark and lepton masses may be given by the following Yukawa interaction and masses,

$$
\begin{aligned}
\mathcal{L} = {}& x_{ij}^u q_i \bar{U}_j H_L^\dagger + \bar{x}_{ij}^u \bar{q}_i U_j H_R^\dagger + M_{ij}^u U_i \bar{U}_j \\
& + x_{ij}^d q_i \bar{D}_j H_L + \bar{x}_{ij}^d \bar{q}_i D_j H_R + M_{ij}^d D_i \bar{D}_j \\
& + x_{ij}^e \ell_i \bar{E}_j H_L + \bar{x}_{ij}^e \bar{\ell}_i E_j H_R + M_{ij}^e E_i \bar{E}_j + \text{h.c.}
\end{aligned}
\tag{2.3}
$$

The gauge charges of the fermions are listed in table 1. Other combinations of fermions are possible as systematically investigated in [12], but to be concrete, we focus on this case in this paper. The parity symmetry restricts the form of x, $\bar{x}$, and M as we will see. See refs. [43–45] for the flavor phenomenology of the setup.

In the limit of $M \gg \bar{x} v_R$, we may integrate out the Dirac fermions and obtain dimension-5 operators of the form

$$
x \frac{1}{M} \bar{x}^t f \bar{f} H_L^{(\dagger)} H_R^{(\dagger)},
\tag{2.4}
$$

where $f = q, \ell$. The SM fermion Yukawa couplings are given by $x \bar{x} v_R / M$. In this limit, the right-handed SM fermions $(\bar{u}, \bar{d}, \bar{e})$ are dominantly from $SU(2)_R$ doublets $\bar{q}$ and $\bar{\ell}$. In the opposite limit $M \ll \bar{x} v_R$, heavy fermions obtain masses of $\bar{x} v_R$ and the SM Yukawas are given by x. The right-handed SM fermions are dominantly from $SU(2)_R$ singlets $\bar{U}$, $\bar{D}$, and $\bar{E}$. Whether or not $M \gg \bar{x} v_R$ can depend on the fermion species and generations; we consider such cases in section 3 to obtain $B - L$ asymmetry. From the collider searches on extra quarks [46–49], a large Dirac mass term $M \gg x v_R$ is required for the first generation unless $v_R \geq 10^8$ GeV.

2.3 Parity and strong CP phase

With the $SU(2)_R$ gauge symmetry, we may impose a space-time parity symmetry. It acts on gauge fields as

$$
G^a_\mu(t, x) \to G^a_\mu(t, -x) \times s(\mu), \qquad B_\mu(t, x) \to B_\mu(t, -x) \times s(\mu),
$$
$$
W^a_{L,\mu}(t, x) \to W^a_{R,\mu}(t, -x) \times s(\mu), \qquad W^a_{R,\mu}(t, x) \to W^a_{L,\mu}(t, -x) \times s(\mu),
$$
$$
s(\mu) = \begin{cases} 1 & \mu = 0 \\ -1 & \mu = 1, 2, 3 \end{cases}
\tag{2.5}
$$

and forbids the CP violating phase in $\theta G \tilde{G}$. The action on fermions is

$$
q(t, x) \to i\sigma_2 \bar{q}^*(t, -x), \ \mathrm{U}(t, x) \to i\sigma_2 \bar{U}^*(t, -x), \ \cdots.
\tag{2.6}
$$

This requires that $\bar{x}_{ij} = x^*_{ij}$ and $M_{ij} = M^*_{ji}$. As a result, the quark mass matrix becomes

$$
\begin{pmatrix} u_i & U_i \end{pmatrix} \begin{pmatrix} 0 & x_{ij}v_L \\ x^*_{ji}v_R & M_{ij} \end{pmatrix} \begin{pmatrix} \bar{u}_j \\ \bar{U}_j \end{pmatrix}.
\tag{2.7}
$$

The determinant of the mass matrix is real, and at the one-loop level, the strong CP phase is not generated from the quark mass [8, 9]. Note also that the Higgs VEVs do not have physical phases, since the phases of the Higgses are gauge degrees of freedom. This is an advantage of the gauge symmetry breaking by H_R and H_L in comparison with that by an $SU(2)_R$ triplet and $SU(2)_R \times SU(2)_L$ bi-fundamentals, where the physical phases of Higgs VEVs must be forbidden by extra symmetries [6, 7, 10, 11].

Two-loop corrections to the phase of the determinant of the quark mass matrix are estimated in refs. [12, 13] for $M > x v_R$ for all quarks and are found to be below the current upper bound. Refs. [8, 9] introduce soft breaking of the parity to the Dirac mass M_{ij}. Although the determinant of the quark mass matrix is real at the tree level, one-loop correction to the phase is generically too large [13]. We assume that the soft breaking in the Dirac mass is suppressed; this is natural given that the Dirac masses are dimension-3 operators while the Higgs masses are dimension-2 operators, and that the Dirac mass may be protected by chiral symmetry.

2.4 Neutrino masses

The masses of SM and right-handed neutrinos, ν and $\bar{N}$, can be obtained in several ways. In one of them discussed in section 2.4.1, right-handed neutrinos can be dark matter.

2.4.1 Majorana mass from dimension-five operators

Neutrino masses can arise from the following two dimension-5 terms,

$$
c^M_{ij} \ell_i \ell_j H^{\dagger 2}_L + c^{M*}_{ij} \bar{\ell}_i \bar{\ell}_j H^{\dagger 2}_R + \mathrm{h.c.},
\tag{2.8}
$$

which can be UV-completed by the see-saw mechanism [50–53]. The sum of the right-handed neutrino masses is given by

$$\sum_i m_{\nu_i} \left(\frac{v_R}{v_L}\right)^2 = 3 \text{ keV} \frac{\sum_i m_{\nu_i}}{60 \text{ meV}} \left(\frac{v_R}{40 \text{ TeV}}\right)^2. \tag{2.9}$$

For experimentally allowed $v_R > 20 \text{ TeV}$, the thermal abundance of the right-handed neutrinos exceed the observed dark matter density. This problem can be avoided by entropy production, and the right-handed neutrinos are good dark matter candidates. The required amount of dilution is

$$D = 40 \frac{\sum_i m_{\nu_i}}{60 \text{ meV}} \left(\frac{v_R}{40 \text{ TeV}}\right)^2 \frac{80}{g_s(T_D)}, \tag{2.10}$$

where T_D is the temperature when the right-handed neutrinos decouple from the thermal bath and g_s is the entropy degree of freedom. This entropy production also dilutes the baryon asymmetry produced at the $\text{SU}(2)_R$ phase transition, and as we will see in section 3.2.2, v_R is bounded from above.

The keV-scale right-handed neutrino dark matter is warm and constrained by the observations of the small-scale structure. Observations of Ly-α forests give a constraint $m_N > \text{few keV}$ [54–57], which is satisfied if $v_R \gtrsim 40 \text{ TeV}$.

The right-handed neutrinos can decay into a SM neutrino and a photon. The decay is induced by a one-loop diagram where N splits into an off-shell W_R and an $\text{SU}(2)_R$ charged lepton, they mix with a W_L and an $\text{SU}(2)_L$ charged lepton respectively, they annihilate into ν, and a photon is attached to an electromagnetically charged particle inside the loop [58–60]. Here the Dirac mass term of $\text{SU}(2)_L \times \text{SU}(2)_R$ singlet fermions (M_{ij} in eq. (2.3)) is necessary for the $\ell - \bar{\ell}$ and $W_L - W_R$ mixing to exist. If those of the third-generation fermions are suppressed, the constraint derived in ref. [60] is relaxed. Indeed, as we will see in section 3, the Dirac mass term for the third-generation charged lepton should be suppressed for successful baryogenesis. This weakens the lower bound on v_R shown in [60] by a factor of $(m_\tau/m_\mu)^{1/2} \simeq 4$, which is already enough to avoid the constraint for $m_N = \text{few keV}$ and $v_R \sim 40 \text{ TeV}$. With a moderately suppressed Dirac mass for the third generation up quark, the constraint is further weakened.

2.4.2 Dirac mass from dimension-five operators

Dirac neutrino masses may arise from the following dimension-5 operator,

$$c_{ij}^D \ell_i \bar{\ell}_j H_L^\dagger H_R^\dagger + \text{h.c.}, \tag{2.11}$$

which can be UV-completed, e.g., by

$$\mathcal{L} = x^\nu \ell H_L^\dagger \bar{S} + x^{\nu*} \bar{\ell} H_R^\dagger S + M^\nu S \bar{S}. \tag{2.12}$$

The right-handed neutrinos have the same mass as the SM ones and behave as dark radiation. For experimentally allowed $v_R > 20 \text{ TeV}$, right-handed neutrinos decouple from the thermal bath before the QCD phase transition, so $\Delta N_{\text{eff}} < 0.3$ and is below the current upper bound [61].

2.4.3 Mojorana mass by radiative inverse seesaw

The right-handed neutrinos can be heavy in the following setup,

$$\chi_i \left(y_{ij}^\chi \ell_j H_L^\dagger + y_{ij}^{\chi*} \bar{\ell}_j H_R^\dagger \right) + m_{\chi,i} \chi_i^2, \tag{2.13}$$

where χ_i are gauge-singlet fermions. After $\mathrm{SU}(2)_R$ and $\mathrm{SU}(2)_L$ breaking, only three linear combinations of the right-handed neutrinos and the SM neutrinos obtain Dirac masses paired with χ_i. Because of $v_R \gg v_L$, the heavy ones are mostly the right-handed neutrinos with masses $y^\chi v_R$.[1] It can decay into a SM Higgs and a lepton doublet without leaving any cosmological impacts.

In this setup, the naive lepton number $\ell(+1)$ and $\bar{\ell}(-1)$ is violated by the coupling with χ. This may lead to the wash-out of asymmetry produced by the $\mathrm{SU}(2)_R$ phase transition. As we will see in the next section, however, this is not necessarily the case. Rather, the violation helps the generation of the $B-L$ asymmetry of SM particles.

The SM neutrinos remain massless. This can be understood by a U(1) symmetry with charges $\chi(-1)$, $\ell(+1)$, and $\ell(+1)$. In the effective theory, after integrating out heavy fields, the neutrino mass, if exists, should be given by a Majorana mass ν^2, but this is forbidden by the U(1) symmetry. Non-zero neutrino masses can be generated by adding a Majorana mass $m_\chi \chi^2$ that explicitly breaks the U(1) symmetry. The neutrino mass is still zero at tree level, and a non-zero neutrino mass arises at one-loop level, as in the radiative inverse-seesaw model [63],

$$m_\nu \sim \frac{(y^\chi)^2}{16\pi^2} \frac{m_\chi v_L^2}{(y^\chi v_R)^2} = \frac{1}{16\pi^2} \frac{m_\chi v_L^2}{v_R^2} \sim 0.1 \text{ eV} \frac{m_\chi}{10 \text{ MeV}} \left(\frac{100 \text{ TeV}}{v_R} \right)^2, \tag{2.14}$$

where we assume $y^\chi v_R > m_W$.

3 Baryogenesis from $\mathrm{SU}(2)_R$ phase transition

In this section, we discuss how a first-order $\mathrm{SU}(2)_R$ phase transition and $\mathrm{SU}(2)_R$ sphaleron processes can produce baryon asymmetry. The essential idea is the same as electroweak baryogenesis; the phase transition proceeds through the formation of bubbles, which expand and provide the deviation from thermal equilibrium. The $\mathrm{SU}(2)_R$ sphaleron process violates the baryon number outside the bubble to create non-zero baryon asymmetry with the aid of some CP violation. The $\mathrm{SU}(2)_R$ sphaleron process becomes ineffective inside the bubbles and the baryon asymmetry is frozen.

There seem to be, however, two apparent obstacles to this idea because of the parity symmetry:

- $B-L$ does not have $\mathrm{SU}(2)_L$ anomaly, so parity symmetry, which exchange $\mathrm{SU}(2)_L$ with $\mathrm{SU}(2)_R$, seems to require $B-L$ not to have $\mathrm{SU}(2)_R$ anomaly. If so, $\mathrm{SU}(2)_R$ phase transition can only create B and L asymmetry with $B-L=0$. Since $\mathrm{SU}(2)_L$ gauge symmetry is still unbroken after the $\mathrm{SU}(2)_R$ phase transition, the produced asymmetries can be washed out by the $\mathrm{SU}(2)_L$ sphaleron process [71].

---

[1]Successful baryogenesis may also be achieved via leptogenesis mechanism from the decaying of the neutral component of $\bar{\ell}$ while v_R is required to be higher than 10^{13} GeV [62].

- The quartic coupling of the $SU(2)_R$-breaking Higgs and the $SU(2)_R$ gauge coupling would be as large as the SM counterparts, so the strong first-order phase transition does not seem to take place.

We discuss how these two obstacles can be avoided in sections 3.1 and 3.2, respectively. Specifically, our solutions to the first obstacle depend on the aforementioned neutrino and charged lepton mass generation mechanism, and use an effective $B - L$ asymmetry coming from the ineffectiveness of some of the interactions and/or $B - L$ violation in the neutrino sector.

CP violation can be obtained in various ways. Note that unlike CP symmetry, parity symmetry does not forbid CP phases but only relates the CP phases of parity partners. To be concrete, we discuss local baryogenesis [32] in section 3.3.

3.1 $B - L$ asymmetry

If the lepton charge of $\bar{\ell}$ is -1, i.e., the $B - L$ charge of it is $+1$, the $B - L$ symmetry does not have $SU(2)_R$ anomaly, so the $SU(2)_R$ sphaleron process does not produce $B - L$ asymmetry. This seems to lead to the washout of baryon asymmetry produced during the $SU(2)_R$ phase transition. However, what lepton charge to be assigned to $\bar{\ell}$ depends on how its asymmetry is transferred into SM particles. In the following, we discuss a few examples where the washout is avoided because of this ambiguity.

3.1.1 Right-handed charged leptons from $SU(2)_R$ doublets

We first consider the case where all of charged-lepton Yukawa interactions are obtained from the dimension-5 operator in eq. (2.4), for which right-handed SM charged leptons $\bar{e}$ are from $SU(2)_R$ doublets $\bar{\ell}$. The asymmetry in $\bar{e}$ can be then transferred into ℓ via the Yukawa coupling. If the scattering between right-handed neutrinos $\bar{N}$ and right-handed electrons $\bar{e}$ via the W_R exchange is also effective, the lepton charge of $\bar{e}$ and $\bar{N}$ should be -1, and the asymmetry is washed out. However, if the W_R exchange decouples before the Yukawa interaction becomes efficient, the wash-out can be avoided.

Light right-handed neutrino. In the neutrino mass model in sections 2.4.1 and 2.4.2, the right-handed neutrino masses are negligible in the early universe. The scattering between $\bar{e}$ and N mediated by W_R is suppressed only by the heavy mass of W_R and decouples at a temperature

$$T_{\rm D} \simeq 10^8 \ {\rm GeV} \left(\frac{v_R}{10^{10} \ {\rm GeV}} \right)^{4/3}.$$
(3.1)

For $v_R > 5 \times 10^7 \ {\rm GeV}$, the W_R exchange decouples before the electron Yukawa becomes effective at a temperature $8.5 \times 10^4 \ {\rm GeV}$ [64]. The asymmetry of $\bar{N}_1$ is not communicated to ℓ, and the total $B - L$ asymmetry of the SM particles is non-zero,

$$\frac{(B-L)_{\rm SM}}{s} = -\frac{n_{\bar{N}_1}}{s} = -\frac{1}{2} \left. \frac{n_{\bar{\ell}_1}}{s} \right|_{T \sim v_R},$$
(3.2)

and the wash-out is avoided [65]. For even higher v_R, the muon and tau Yukawa interactions are also out of equilibrium when the W_R exchange decouples, so $B - L$ asymmetry becomes larger.

Heavy right-handed neutrino. In the neutrino mass model in section 2.4.3, the right-handed neutrinos can be heavy and their abundance is suppressed for $T \ll y^\chi v_R$. The scattering rate between $\bar{N}_1$ and $\bar{e}_1$ is suppressed not only by the large W_R mass but also by the Boltzmann factor $\exp(-y^\chi v_R/T)$,

$$\Gamma \sim \frac{T^{3/2}(y^\chi v_R)^{7/2}}{8\pi v_R^4} \times \exp\left(-\frac{y^\chi v_R}{T}\right). \tag{3.3}$$

For $y^\chi = O(1)$, the W_R exchange decouples before the electron Yukawa gets into equilibrium if $v_R \gtrsim 2 \times 10^6$ GeV.

Since the asymmetry in $\bar{N}_1$ is suppressed by the Boltzmann factor unlike the setup with light right-handed neutrinos, one may worry that the total $B - L$ asymmetry is also exponentially suppressed; this may not the case because of the $B - L$ violation by y^χ, which can process the asymmetry produced by the SU(2)$_R$ phase transition into non-zero $B - L$ asymmetry. (This is analogous to the conversion of the asymmetry produced by the GUT baryogenesis, where $B - L = 0$, into non-zero $B - L$ asymmetry by lepton-number violation [66–70].) The $B - L$ violation generically leads to the complete wash-out of all asymmetries. However, if y^χ is nearly diagonal in the charged lepton flavor basis,[2] the following symmetry, which we call U(1)$_{L_1'}$, is approximately preserved before the electron Yukawa gets into thermal equilibrium at the classical level: $\ell_1(+1)$, $\bar{\ell}_1(+1)$, $\chi_1(-1)$. $B/3 - L_1'$ is an approximate symmetry without SU(3)$_c \times$ SU(2)$_L$ gauge anomaly, but has SU(2)$_R$ anomaly and can be produced by the SU(2)$_R$ phase transition. Using the method in [71], one can show that the standard $B - L$ charge $(\bar{e}_1(+1), \ell_1(-1), \dots)$ indeed becomes non-zero. U(1)$_{L_1'}$ is explicitly broken by the electron Yukawa,[3] but by the time it becomes effective, $\bar{e}_1$ no longer communicates its charge with $\bar{N}_1$ via the W_R exchange and the $B - L$ violation by y^χ is ineffective. Because of the standard $B - L$ charge conservation, the baryon asymmetry remains non-zero.

3.1.2 A right-handed charged lepton from an SU(2)$_R$ singlet

The scenarios in section 3.1.1 require large v_R and there are no light enough particles to be produced at near future colliders. Successful scenarios with lower v_R exist if the charged lepton masses have the following structure,

$$\begin{aligned}\mathcal{L} = x_{ij}^e \ell_i \bar{E}_j H_L + x_{ij}^{e*} \bar{\ell}_i E_j H_R + M_{ij}^e E_i \bar{E}_j \quad (i, j = 1, 2) \\ + y_\tau \ell_3 \bar{E}_3 H_L + y_\tau^* \bar{\ell}_3 E_3 H_R + \text{h.c.},\end{aligned} \tag{3.4}$$

which may be ensured by an approximate U(1) symmetry with charges $\ell_3(1)$, $\bar{\ell}_3(1)$, $E_3(-1)$, and $\bar{E}_3(-1)$. For this structure, the lepton charge of $\bar{\ell}_3$ and E_3 are not necessarily -1 and

---

[2]The neutrino mixing can come from non-diagonal m_χ.

[3]The symmetry is also explicitly broken by the Majorana mass term m_χ, but it is still small enough and the wash-out by this explicit breaking is ineffective.

+1 and the wash-out may be avoided as described below. We call the two components in $\bar{\ell}_3$ as $\bar{N}_3$ and $\bar{\tau}'$, and E_3 as τ'. Note that there is no M_{3i}^e or M_{i3}^e in eq. (3.4).

Because of the parity symmetry, τ' mass is predicted to be $m_\tau v_R / v_L$. The collider signature of τ' is discussed in section 4. The mechanisms we discuss below works also for the case where some of the first two generations have the structure of a vanishing Dirac mass, $M_{1i}^e = 0$ or $M_{2i}^e = 0$, for which even lighter new fermions with masses $y_e v_R$ or $y_\mu v_R$ are predicted. To be conservative, we assume that only τ' is light.

Light right-handed neutrino. For the neutrino mass models in sections 2.4.1 and 2.4.2, the interaction of $\bar{\ell}$ through the neutrino mass operators is ineffective because of the smallness of the neutrino mass. With the structure of charged leptons in eq. (3.4), among the asymmetry of $\bar{\ell}_{1,2,3}$ created by the $SU(2)_R$ sphaleron process, only that of $\bar{\ell}_{1,2}$ is transferred into $SU(2)_L$ charged particles. Therefore, the total $B - L$ asymmetry of the SM particles is non-zero,

$$\frac{(B-L)_{\text{SM}}}{s} = -\left.\frac{n_{\bar{\ell}_3}}{s}\right|_{T \sim v_R}. \tag{3.5}$$

The same way of obtaining non-zero baryon asymmetry is also employed in a model of baryogenesis from axion rotation, called axiogenesis [72], in [65].

In this scenario, it is crucial that the transfer of the asymmetries in $\bar{\ell}_3$ and E_3 into other leptons is negligible, since otherwise the wash-out of the asymmetry occurs. Let us derive the bound on the parameters of the theory, taking the mass term $M_3 \bar{E}_3 E_3$ as an example. Since the scattering rate via M_3 is exponentially suppressed at $T < m_{\tau'}$, the ratio between the scattering rate and the Hubble expansion rate is maximized at $T \sim m_{\tau'}$. A care must be taken in the choice of basis. Instead of choosing the basis where the Yukawa interaction y_τ is diagonal, we may rotate $(\bar{E}_3, \bar{\tau}')$ to remove M_3 and define the asymmetry in this basis. We should take the basis with a smaller transfer late [73, 74], since it is enough to have one basis in which the charges are separated with each other. It turns out that we shall use the basis with a diagonal Dirac mass term when $y_\tau T < m_{\tau'}$, which is indeed the case after $SU(2)_R$ phase transition since $m_{\tau'} = y_\tau v_R$. This can be also understood from the thermal mass given by the Yukawa interaction $y_\tau T$ being smaller than $m_{\tau'}'$, so that the Hamiltonian of quasi-particles on the thermal background is closer to a diagonal one in the basis where the Dirac mass is diagonalized. In this basis, the charge transfer is induced by a Yukawa interaction $y_\tau M_3 / m_{\tau'}$. We require that

$$\alpha_2 y_\tau^2 \frac{M_3^2}{m_{\tau'}^2} T < H(T = m_{\tau'}) \longrightarrow M_3 < 20 \text{ MeV} \left(\frac{v_R}{100 \text{ TeV}}\right)^{3/2}. \tag{3.6}$$

Even if this condition is violated, the washout is avoided if the scattering between $\bar{\tau}'$ and $\bar{N}_3$ via the W_R exchange are ineffective when the scattering by M_3 becomes effective. However, the W_R exchange is indeed effective at $T \sim m_{\tau'}$, so the upper bound in eq. (3.6) is applicable.

Heavy right-handed neutrino. We next consider the neutrino mass model in section 2.4.3. If the coupling y_{ij}^χ is not nearly diagonal in the charged lepton mass eigenbasis,

all possible lepton symmetries are violated, and the asymmetry produced by the $SU(2)_R$ phase transition is washed out.

On the other hand, if y_{ij}^χ is nearly diagonal, although the first and second-generation lepton symmetry is violated, the third-generation leptons preserve the following symmetry which we call $U(1)_{L_3'}$; $\ell_3(+1)$, $\bar{E}_3(-1)$, $\bar{\ell}_3(+1)$, $E_3(-1)$, and $\chi_3(-1)$. With this charge assignment, $B/3 - L_3'$ has $SU(2)_R$ anomaly and hence can be produced by the $SU(2)_R$ phase transition. As the temperature drops below the right-handed neutrino mass $y^\chi v_R$ and the τ' mass, the third-generation lepton asymmetry is stored dominantly in $\bar{E}_3$ and ℓ_3, namely, the tau and tau neutrino. Because of the violation of the standard $B - L$ symmetry by y^χ, the total $B - L$ asymmetry of the SM particles becomes non-zero.

L_3'-breaking parameters should be sufficiently small to avoid washout. Let us again take M_3 as an example. Note that the washout is avoided even if the scattering or decay involving M_3 becomes effective at a low temperature, as long as the scattering between τ' and N_3 has already decoupled by that time. This is because the following standard lepton symmetry is preserved: $\ell_3(+1)$, $\bar{E}_3(-1)$ $\bar{\tau}'(-1)$, $E_3(+1)$. One can show that this standard $B - L$ charge indeed becomes non-zero. At $T \ll y^\chi v_R$, the scattering rate between $\bar{\tau}'$ and $\bar{N}_3$ is suppressed not only by the large W_R mass but also by the Boltzmann factor $\exp(-y^\chi v_R/T)$,

$$\Gamma \sim \frac{T^{3/2}(y^\chi v_R)^{7/2}}{8\pi v_R^4} \times \exp\left(-\frac{y^\chi v_R}{T}\right). \tag{3.7}$$

For example, for $v_R = 20 - 100\,\text{TeV}$ and $y^\chi = 1$, the scattering decouples at $T_d = 0.7 - 4\,\text{TeV}$, which is above $m_{\tau'}$. The upper bound on M_3 is given by

$$\alpha_2 y_\tau^2 \frac{M_3^2}{m_{\tau'}^2} T \lesssim H(T = T_d) \longrightarrow M_3 < 40\,\text{MeV} \left(\frac{T_d}{4\,\text{TeV}}\right)^{1/2} \left(\frac{v_R}{100\,\text{TeV}}\right). \tag{3.8}$$

3.2 Strong first-order phase transition

The SM Higgs coupling is about 0.13 around the weak scale. If the quartic coupling of H_R is of this order and H_R only has the Yukawa couplings in eqs. (2.1) and (2.3) and gauge interactions, strong first-order phase transition cannot occur. Indeed, as in the SM, for $g_R = g_L \simeq 0.65$, the $SU(2)_R$ Higgs quartic coupling must be smaller than 0.017 [75–80] for a strong first-order phase transition to occur for vanishing fermion Yukawa contributions, and with heavy top mass the phase transition strength should be further suppressed because of the positive correction to the quartic coupling [81, 82]; see also appendix A.

In the rest of this subsection, we discuss how the $SU(2)_R$ phase transition can be of strong first order. In the models we discuss, no hierarchy problems beyond that of H_L and H_R are introduced. The effective thermal potential is computed up to one-loop level, as described in appendix A. For marginally SFOPT, high-temperature expansion shows a great agreement with the full form. Since we are aiming at finding the boundary of the parameter space to achieve SFOPT, we use the high-temperature expansion throughout this subsection to simplify the computation.
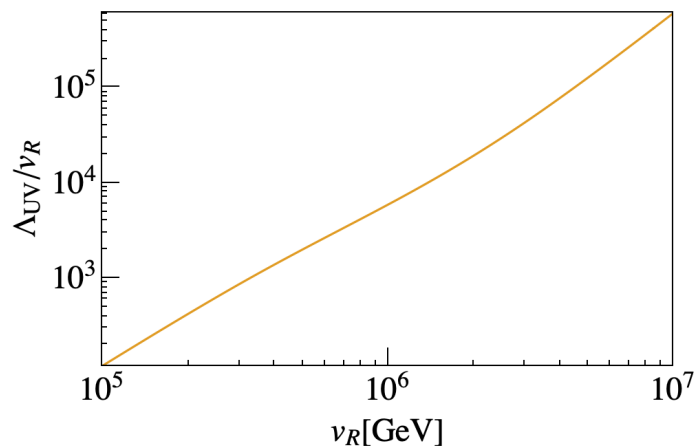
Figure 1. Required scale of new physics Λ_{UV} to avoid the instability of the Higgs potential for extra leptons with a mass of $1\,\mathrm{TeV}$. Here the extra Yukawa couplings are chosen to be the minimal value to achieve the SFOPT.

3.2.1 Running quartic coupling

With the hierarchy $v_L \ll v_R$, it is possible to utilize the running of the quartic coupling. The SM Higgs quartic coupling becomes smaller at high energy scales because of the quantum correction from Yukawa couplings. If there are no extra particles contributing to the β-function of the quartic coupling, the quartic coupling λ_R becomes smaller than 0.015 at around 10^8 GeV. We computed the effective potential for H_R at different energy scales with corresponding running couplings, and found that a SFOPT can be achieved for $v_R > 2 \times 10^8$ GeV. Here and hereafter, we assume that the quartic coupling $|H_L|^2|H_R|^2$ is negligible. If not, the threshold correction to $|H_L|^4$ at the scale v_R via the H_R exchange makes the SM Higgs quartic coupling $|H_L|^4$ smaller than $|H_R|^4$ and the lower bound on v_R becomes stronger.

If H_L has $O(1)$ Yukawa couplings to new fermions, the running becomes faster, and a strong first-order phase transition can occur for much smaller v_R. As an example, we add extra fermions

$$\psi = (\mathbf{1}, \mathbf{2}, \mathbf{1}, -\frac{1}{2}), \quad \bar{\psi} = (\mathbf{1}, \mathbf{2}, \mathbf{1}, \frac{1}{2}), \quad \Psi = (\mathbf{1}, \mathbf{1}, \mathbf{1}, 0), \tag{3.9}$$

with Yukawa couplings $y_\psi H_L^\dagger \psi \Psi$ and $\bar{y}_\psi H_L \bar{\psi} \Psi$ and mass terms $m_\psi \psi \bar{\psi}$ and $m_\Psi \Psi^2$. The corresponding $SU(2)_R$ charged partners and their interactions are also introduced. This extra Yukawa coupling quickly makes the quartic coupling small enough to achieve SFOPT. The required Yukawa coupling y_ψ to obtain a small enough λ_R depends on the masses of these extra fermions. Their lightness does not introduce extra hierarchy problems because of the protection of fermion masses by chiral symmetry.

On the other hand, a large extra Yukawa coupling may introduce the problem of the instability of the potential. With a large extra Yukawa coupling, the quartic coupling at a large Higgs field value quickly becomes negative. The tunneling rate from the metastable point $\langle H_R \rangle = v_R$ to infinity can be computed via the pseudo-bounce action method [83]. We

use the zero-temperature effective potential $V_{T=0}$ in appendix A to compute the tunneling action. For an escape point with a large field value, the pseudo-bounce action becomes smaller, making the tunneling more likely to happen. A large enough escape point thus always leads to instability. The value of the escape point that gives a small enough bounce action is regarded as a UV scale Λ_{UV} below which the modification of the Higgs potential by new physics is required. In figure 1, we show $\Lambda_{\mathrm{UV}}/v_R$ as a function of v_R, with the extra Yukawa coupling chosen to be the minimal value achieving SFOPT. The extra fermion assisting the running is assumed to have a mass of 1 TeV.

We cannot argue that SFOPT can be achieved for $v_R < 10^5$ GeV. Even for the TeV-scale extra leptons, the required Yukawa coupling y_ψ is order one, which is close to that of the top quark at the EW scale. For such a large Yukawa coupling, similar to the SM EW phase transition analyzed in ref. [81], the result of 1-loop perturbative computation highly depends on approximation methods and renormalization schemes/scales. Some of them deviate from the result of lattice simulation significantly. More advanced computation techniques such as dimension reduction, and computation up to higher-order loops are required in such a case [84–87], which is beyond the scope of this paper. For a discussion of the theoretical uncertainties of the computation, see appendix A.

We comment on the uncertainty from the top quark mass, to which the running is sensitive. We used the central value $m_t = 172.69$ GeV [88]. If the top quark mass shifts by 1 GeV, the minimal v_R achieving SFOPT in the minimal model changes by a factor of 10. The prediction for $\Lambda_{\mathrm{UV}}/v_R$ in figure 1, however, does not change, since the shift of the top quark mass can be absorbed into the shift of the free parameters y_ψ and $\bar{y}_\psi$.

3.2.2 Extra scalars

A strong first-order phase transition may be also achieved via extra scalar fields that couple to Higgses, which have been intensively investigated in the literature in the context of electroweak phase transition. Those models can be categorized into two types: the couplings may enhance the cubic term (see appendix A) via loop effects, or modify the (effective) tree-level quartic coupling directly via mixing with the Higgs. The former includes, for example, the MSSM [18–23], a real Z_2-even singlet scalar [16, 17], and so forth. The latter includes the 2HDM model [26–28], a real Z_2-odd singlet scalar [25], the NMSSM [24], a complex singlet scalar [29], and so forth. For a review, see [89]. Here we analyze an example of real singlet scalars investigated in [30, 31], where the singlet scalars are naturally light and no extra hierarchy problem is introduced.

We introduce two extra scalar singlets S_L and S_R. (One singlet case does not work as we explain later.) The tree-level potential is

$$
\begin{aligned}
V_0 = {}& -\frac{1}{2}\mu_{H_L}^2 h_L^2 - \frac{1}{2}\mu_{H_R}^2 h_R^2 + \frac{1}{4}\lambda(h_L^4 + h_R^4) + \frac{1}{4}\lambda_{\mathrm{LR}} h_L^2 h_R^2 \\
& + \frac{1}{2}\mu_S^2(S_L^2 + S_R^2) + \frac{1}{2}A S_L(h_L^2 - 2v_L^2) + \frac{1}{2}A S_R(h_R^2 - 2v_R^2) \\
& + \frac{1}{2}A' S_L(h_R^2 - 2v_R^2) + \frac{1}{2}A' S_R(h_L^2 - 2v_L^2).
\end{aligned}
\tag{3.10}
$$

S_L and S_R enjoy a shift symmetry $S_{L,R} \to S_{L,R} + \delta_{L,R}$ that is softly broken by the mass terms and the trilinear couplings. As long as $A, A' < \mu_S$, the lightness of $S_{L,R}$ is natural.

Let us for now take A' to be zero and discuss the effect of non-zero A' later. For given field values of h_L and h_R, the potential is minimized at

$$\langle S_{L,R} \rangle = \frac{A}{2\mu_S^2}(h_{L,R}^2 - 2v_{L,R}^2).$$ (3.11)

The potential along this trajectory is

$$V_0(h_L, h_R, \langle S_L \rangle, \langle S_R \rangle) = -\frac{1}{2}\mu_{H_L}^2 h_L^2 - \frac{1}{2}\mu_{H_R}^2 h_R^2 + \frac{1}{4}\left(\lambda - \frac{A^2}{2\mu_S^2}\right)(h_L^4 + h_R^4) + \frac{1}{4}\lambda_{LR} h_L^2 h_R^2.$$ (3.12)

One can see that the effective quartic coupling λ_{eff} receives a tree-level modification, $\lambda_{\text{eff}} = \lambda(v_R) - A^2/(2\mu_S^2)$, and the phase transition strength is enhanced.

The lower bound on A to achieve a SFOPT is translated into a lower bound on $S_L - h_L$ mixing, which is shown by the lower blue-shaded regions in figure 2. We take into account the running of A and λ from the EW scale to v_R. We take λ_{LR} to be zero; non-zero λ_{LR} gives a tree-level threshold correction to the quartic coupling of H_L via the H_R exchange and the required A becomes larger. λ_{LR} induced by $U(1)_X$ interaction is negligible. Since the quartic coupling λ is smaller at v_R than at the EW scale, the required magnitude of A to achieve the SFOPT becomes smaller and thus mixing angle is smaller than that in refs. [30, 31]. In the upper blue-shaded region, $\lambda - A^2/(2\mu_S^2)$ at v_R is negative, and the potential is unstable. Here we again assume $m_t = 172.69$ GeV [88]. We found that the prediction for the mixing angle shifts by 5% for the shift of the top quark mass by 1 GeV. We discuss the uncertainties in the computation of the electroweak-like phase transition in appendix A. The result agrees with the conclusion of refs. [82, 90] that 2-loop computation gives a stronger phase transition. Thus, our prediction in figure 2, which is based on the 1-loop potential with high-temperature expansion, is regarded as a conservative one.

Here it is crucial that the mass of S is below the EW scale and cannot be integrated out. Otherwise, the effective coupling of H_L corrected by A is no longer an effective one. Rather, it is the actual Higgs coupling in the effective theory after integrating out S that determines the SM Higgs mass. As a result, the quartic coupling at the energy scale above the S mass becomes larger and the $SU(2)_R$ phase transition cannot be a SFOPT unless v_R is above 10^8 GeV.

The model is further constrained by direct searches for the singlet scalars. The mixing between S_R and the SM Higgs is suppressed by λ_{LR}, so we focus on S_L that mixes with the SM Higgs and can be probed in various ways. S_L heavier than a few GeV can be probed in collider experiments by direct production of S_L. A search up to 100 GeV was performed assuming that S_L decays into SM fermions, with $S_L \to b\bar{b}$ providing the most stringent bound [91]. A search independent of the decay mode of S_L via $e^+ e^- \to Z S_L$ is also performed [92, 93]. (This search is also applicable even if S_L dominantly decays into a dark sector.) We compare all the bounds mentioned above and choose the most stringent one for each mass, leading to the magenta-shaded region of figure 2.

This scalar can be also searched via an extra decay channel $h \to S_L S_L$ of the SM Higgs. This decay channel was searched at LHC for various final states. Ref. [94] summarizes all

current searches and derives a combined exclusion curve, using a proper branching ratio for S_L decaying into SM fermions. The prospect of future search is discussed in section 4.4. In figure 2, though the current exclusion curve is outside the plotted range, we show the future projection curve with dashed lines.

S_L with a mass below a few GeV can be probed by rare meson decay (see [95] for review, and see [96] for recent updates.) LHCb performed a search with $B^+ \to K^+ S_L(\mu^+\mu^-)$ [97] and $B^0 \to K^0 S_L(\mu^+\mu^-)$ [98] for 200 MeV $\le m_S \le 4$ GeV. The scalar mass at the MeV scale is not excluded by the direct searches for S_L, but is excluded by the cosmological problem of S_R as explained later.

Now let us discuss the effect of A'. Without loss of generality we take $A' < A$, otherwise we can rename $S_{L,R}$ as $S_{R,L}$. The most important effect of this coupling is to give a tree-level threshold correction to the mass of S_L via h_R exchange;

$$\mu_S^2 \to \mu_{S_L}^2 = \mu_S^2 - \frac{A'^2}{2\lambda(v_R)}$$

$$\mu_S^2 \to \mu_{S_R}^2 = \mu_S^2 - \frac{A^2}{2\lambda(v_R)} = \mu_S^2 \frac{\lambda_{\text{eff}}}{\lambda(v_R)} \tag{3.13}$$

That means that for a given $\mu_{S_L}^2$, μ_S^2 is larger by $A'/(2\lambda(v_R))$. To achieve SFOPT, a larger A is required to enhance the tree-level correction to λ_{eff}, i.e., $-A^2/(2\mu_S^2)$. The allowed parameter space in (m_S, θ) for SFOPT is shifted above. For example, if A' is not smaller than A by a factor of 3, the allowed parameter space for SFOPT is excluded by collider experiments. This is also the reason why the model with a single S and a coupling $AS(h_L^2 + h_R^2)$ does not work.

The MeV-scale mass is probed by rare kaon decay [99, 100] and negative ΔN_{eff} [61, 101]. Large mixing with h_L is excluded by the rare kaon decay because of the large branching fraction of $K \to \pi S$, while small mixing is excluded by the decay of S into electrons after neutrinos decouple, which makes neutrinos relatively cooler. These constraints on S_L are satisfied for $m_{S_L} < 20$ MeV, but not once the cosmology of S_R is taken into account. S_R couples with H_R and is thermalized when $T \sim v_R$. If A' is small, the mixing of S_R with h_L is small, so S_R decouples from the bath when it is relativistic and decays much after neutrinos decouple and S_R becomes non-relativistic. This leads to a too large negative ΔN_{eff}. If A' is of the same order as A, S_R mixes with h_L, and the ΔN_{eff} constraint can be evaded. However, the threshold correction to $\mu_{S_L}^2$ discussed above shifts the allowed parameter space for SFOPT above, and the constraint from the rare kaon decay excludes it. Combining all these requirements, we found no allowed parameter.

3.3 Example of CPV: local baryogenesis

In this paper, we consider local baryogenesis for its simplicity and effectiveness, following the proposal in [32] for the electroweak phase transition. We first review the local baryogenesis in a general way for the thick-wall regime where the wall is thicker than the mean free-path of particles $\sim (\alpha_R T)^{-1}$. Indeed, for the models using the running quartic or the extra singlet scalar, we find that the wall thickness is around $100/T$. We then discuss two specific models.
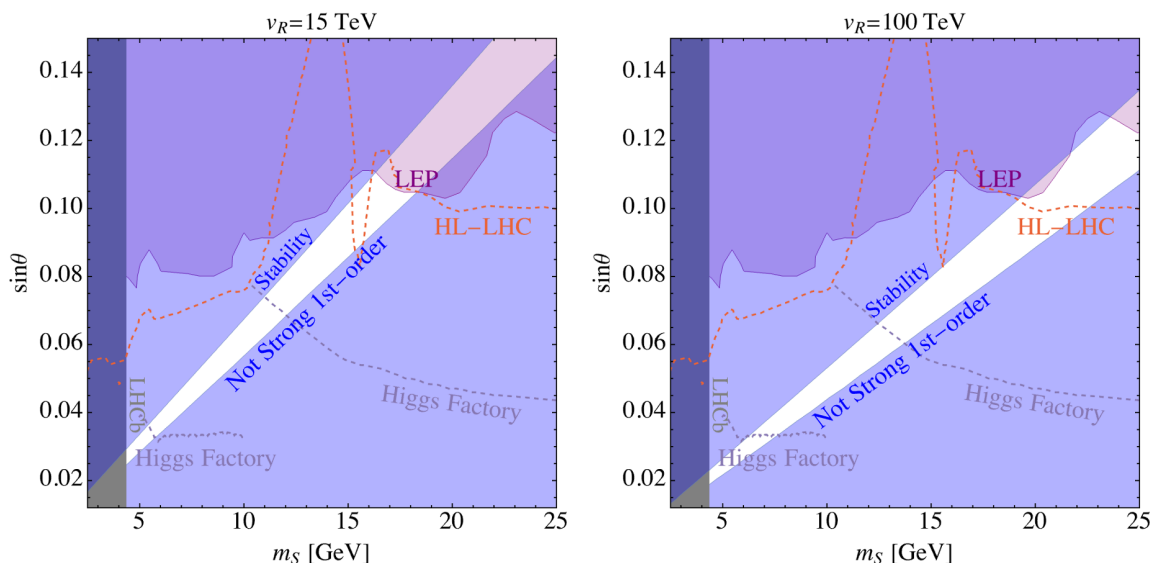
Figure 2. Parameter space for the scalar extension in eq. (3.10). Blue-shaded region: excluded by the SFOPT condition and stability requirement. Magenta-shaded region: LEP constraint from direct production. Orange-shaded region: LHC constraint from Higgs exotic decay. Gray shaded region: LHCb constraint from a rare B-meson decay. White space: allowed parameter space. Orange dashed line: HL-LHC prospect for extra scalar search via Higgs exotic decay. Purple dashed line: Higgs factory prospects for extra scalar search via Higgs exotic decay.

If H_R couples to heavy $\mathrm{SU}(2)_R$ charged fermions directly or indirectly and CP is violated by the coupling or mass of the fermions, the $\mathrm{SU}(2)_R$ theta term may depend on H_R,

$$\frac{g^2}{32\pi^2}\theta(H_R)W_R\tilde{W}_R. \tag{3.14}$$

We follow the method in [32] to calculate the baryon asymmetry. During the FOPT by bubble nucleation, spacial points that are initially outside an expanding bubble are later swept by the bubble wall and get inside the bubble. During this transition, while the spacial points are on the bubble wall, sphaleron processes produce asymmetry of fermions with $\mathrm{SU}(2)_R$ charges via quantum anomaly, and the processes become ineffective inside the bubble. In the thick-wall regime, the H_R field value changes gradually across the bubble wall and the asymmetry of particles may be computed by thermodynamics and small deviation from the local thermal equilibrium. The change of the field value of H_R across the bubble wall gives a time-dependent θ term and hence a bias between the $\mathrm{SU}(2)_R$ sphaleron transition increasing asymmetry and that decreasing asymmetry. The imbalance between the two processes produces asymmetry of fermions. (The produced asymmetry gives an opposite bias, but it is negligible unless the asymmetry reaches an equilibrium value.)

As discussed in section 3.1, the final baryon number is determined by the lepton number carried by the new charged lepton $\bar{\ell}_3$ and E_3. The $\mathrm{SU}(2)_R$ sphaleron process produces the asymmetry of $\bar{\ell}_3$ as described above,

$$\dot{n}_{\bar{\ell}_3} = \frac{\Gamma_{\mathrm{Rs}}}{T^3}\dot{\theta}T^2, \tag{3.15}$$

where Γ_{Rs} is the $SU(2)_R$ sphaleron transition rate. This equation can be solved by performing an integration over time on the right-hand side along the wall profile. When the Higgs field value is sufficiently small, the sphaleron transition rate is given by [102]

$$\Gamma_{\text{Rs}} = \kappa \alpha_R^5 T^4, \tag{3.16}$$

where $\kappa \simeq 20$. The sphaleron rate receives an exponential suppression when the field value of H_R becomes large enough. By the time this occurs, $\theta(H_R)$ changes by $\delta\theta$. Then the baryon asymmetry produced by the $SU(2)_R$ phase transition normalized by the entropy density is given by

$$Y_B = \frac{n_B}{s} = \frac{28}{79}\frac{1}{s}\kappa\alpha_R^5 T^3 \delta\theta = 8.6 \times 10^{-11}\frac{\delta\theta}{0.02}. \tag{3.17}$$

One can see that the observed baryon asymmetry can be obtained even with $\delta\theta \ll 1$.

In the neutrino mass model in section 2.4.1, right-handed neutrinos can be dark matter if entropy production given by eq. (2.10) occurs. The entropy production also dilutes baryon asymmetry, so larger $\delta\theta$ is required. This gives an upper bound on the sum of right-handed neutrino mass,

$$\sum_i m_{N_i} < 10 \text{ keV} \times \frac{\delta\theta_{\max}}{\pi}. \tag{3.18}$$

Here we take the maximal $\delta\theta$, $\delta\theta_{\max}$, to be π. If there are multiple heavy $SU(2)_R$ charged fermions in the UV completion of the local operator in eq. (3.14), $\delta\theta_{\max}$ can be larger. Unless the number of those heavy fermions is large, the warmness of dark matter can be observed by future observations of 21cm lines [103]. The upper bound on the masses of right-handed neutrinos also gives an upper bound on v_R,

$$v_R \leq 70 \text{ TeV} \left(\frac{60\text{meV}}{\sum_i m_{\nu_i}}\right)^{1/2} \left(\frac{g_s(T_D)}{80}\right)^{1/2} \left(\frac{\delta\theta_{\max}}{\pi}\right)^{1/2}. \tag{3.19}$$

Now we discuss more specific models, which may be subject to stronger constraints. We consider the following dimension-6 CP-odd operator [32],

$$\frac{g^2}{32\pi^2 M^2}|H_R|^2 W_R \tilde{W}_R. \tag{3.20}$$

The parity symmetry does not forbid this CP-odd operator and only requires another dimension-6 operator composed of H_L and W_L with the same strength. The operator may be UV-completed by, e.g., the following parity-symmetric interactions and masses,

$$yH_R L'\eta + \lambda H_R^\dagger \bar{L}'\eta + m_L L'\bar{L}' + \frac{1}{2}m_\eta \eta^2$$
$$+ y^* H_L \bar{L}\eta + \lambda^* H_L^\dagger L\eta + m_L^* L\bar{L} + \text{h.c.}, \tag{3.21}$$

with the $SU(2)_L \times SU(2)_R \times U(1)_X$ charges of the fermions given by $L'(\mathbf{1}, \mathbf{2}, -1/2)$, $\bar{L}'(\mathbf{1}, \mathbf{2}, -1/2)$, $\eta(\mathbf{1}, \mathbf{1}, 0)$, $L(\mathbf{2}, \mathbf{1}, 1/2)$, and $\bar{L}(\mathbf{2}, \mathbf{1}, 1/2)$. The parity symmetry requires that m_η is real, but the physical CP phase $\arg(y\lambda/(m_L m_\eta))$ is in general non-zero.

We make an approximation that the sphaleron rate is given by eq. (3.16) when $m_{W_R}(H_R) < \sigma \alpha_R T$ and zero for $m_{W_R}(H_R) > \sigma \alpha_R T$. Here σ is a constant that can be estimated from the simulation in ref. [102], and we obtain $\sigma \simeq 3$. Putting all information together, the final baryon-to-entropy ratio is given by

$$Y_B = \frac{n_B}{s} = \frac{28}{79} \frac{1}{s} \frac{4\Gamma_{\rm sph} \sigma^2 \alpha_R^2 T}{M^2 g^2} \bigg|_{T=T_n} \simeq 8.9 \times 10^{-11} \left(\frac{1.7 T_n}{M}\right)^2. \tag{3.22}$$

The observed baryon asymmetry $Y_B \simeq 8.7 \times 10^{-11}$ can be achieved for M slightly above T_n. This justifies the use of the dimension-6 operator; the masses or heavy particles in UV-completion of the operator ($\bar{L}$, $\bar{L}'$, and η in the above example) can be above T_n so that they may be indeed integrated out. The setup, however, cannot accommodate the dilution necessary for the model with right-handed neutrino dark matter while satisfying $M > T_n$.

In the model with extra scalars, the following dimension-5 operator can achieve local baryogenesis [31],[4]

$$\mathcal{L} = \frac{\alpha_R}{8\pi} \frac{S_R W_R \tilde{W}_R}{M}. \tag{3.23}$$

This operator may be UV-completed by identifying S with a pseudo Nambu-Goldstone boson with a decay constant $\sim M$ and weak anomaly. Since the shift of the field value of S_R is around $\Delta S_R \simeq A \Delta h_R^2/(2\mu_S^2)$, the baryon asymmetry is given by eq. (3.22) multiplied by $MA/(2\mu_S^2)$. Around the allowed parameter space in figure 2, we always have $A/\mu_S \simeq 0.3$. Thus we obtain

$$Y_B \simeq 8.7 \times 10^{-11} \left(\frac{v_R}{20 \text{ TeV}}\right) \left(\frac{T_n}{0.2 v_R}\right)^2 \left(\frac{40 v_R}{M}\right) \left(\frac{10 \text{ GeV}}{\mu_S}\right). \tag{3.24}$$

Here we normalized T_n by the value we find by computing the bounce action, $T_n \simeq 0.2 v_R$. The smallness of μ_S causes the large shift of the field value of S_R during the phase transition and strongly enhances the generated baryon asymmetry. As a result, M may be much above T_n.

In deriving the parameter space achieving SFOPT by computing the bounce action, we assume S^2 and $S|H|^2$ terms and neglect higher-order terms. This requires that the shift of S from the SU(2)$_R$ symmetric point to the escape point in the bounce solution be smaller than M, since otherwise higher order terms in general become comparable to the terms we consider. We find that the shift is about $T_n/4$, which is indeed much smaller than M.

4 Signals

In this section, we discuss the experimental signals of the model.

---

[4]We assume that the singlets do not couple to the SU(3)$_C$ field strength, since otherwise $\langle S_L \rangle \neq \langle S_R \rangle$ generate a non-zero strong CP phase.

4.1 New gauge bosons

The left-right symmetric model predicts a new W_R gauge boson and a Z' gauge boson. Their masses are given by

$$
\begin{aligned}
m_{W_R} &= m_W \frac{v_R}{v_L} = 6.5 \text{ TeV} \frac{v_R}{15 \text{ TeV}}, \\
m_{Z'} &= m_Z \frac{v_R}{v_L} = 7.4 \text{ TeV} \frac{v_R}{15 \text{ TeV}}.
\end{aligned}
\tag{4.1}
$$

The new gauge bosons couple with SM leptons and quarks, and thus can be searched for by collider experiments for various final states, including lepton+MET, jets, di-lepton, etc. The current limit from the W_R search is more stringent than that of Z'. The W_R boson with a mass below 6.0 TeV is excluded by the search for di-electron final states [104], corresponding to $v_R = 14.1$ TeV. The high-luminosity LHC (HL-LHC) can detect the W_R boson with a mass up to 7.9 TeV [105], corresponding to $v_R = 18.6$ TeV.

4.2 New charged particle

As is discussed in section 3.1, a non-zero $B - L$ asymmetry can be produced if $v_R > 10^6$ GeV or the charged lepton mass has the structure in eq. (3.4). While the former scenario has no collider signatures, the latter predicts a parity partner of the tau lepton with a mass

$$
m_{\tau'} = m_\tau \frac{v_R}{v_L} \simeq 150 \text{ GeV} \frac{v_R}{15 \text{ TeV}}
\tag{4.2}
$$

and a hypercharge of unity. The mass is correlated with the masses of the new gauge bosons W_R and Z'. It is possible that the other two generations of leptons have the structure of the vanishing Dirac mass term M_{ij}, for which case even lighter charged leptons are predicted. To be conservative, we consider the case where only τ' is light and discuss how to probe it in collider experiments.

τ' is pair-produced by the hypercharge gauge interaction at colliders, whose cross section is computed in, e.g., [106, 107]. The decay channel of τ' depends on how the right-handed neutrino masses are obtained. When they are obtained via a dimension-5 Majorana or Dirac mass operator, N is light so τ' promptly decays into N via an off-shell W_R boson. The collider signals are then $e^+ e^-$, $\mu^+ \mu^-$, $e^+ \mu^-$, $e^- \mu^+$, $e + 2$ jets, $\mu + 2$ jets, or 4 jets, all accompanied by missing energy from right-handed neutrinos. Note that τ final states are absent since the SM right-handed tau is $\text{SU}(2)_R$ singlet. The signal resembles that of pair-production of charginos decaying into a neutralino and W. Comparing the upper bound on the cross section provided in the HEPData version of [108] with the production cross section of hyper-charged fermions, we find that there is no LHC constraint. Only the LEP bound of $m_{\tau'} > 100$ GeV [109] is applicable.

When the right-handed neutrino mass is generated by eq. (2.13), the decay channel depends on whether the right-handed neutrino is heavier than τ'. If N_3 is lighter than τ', τ' will decay to N_3 and emits an off-shell W_R gauge boson. For m_{N_3} below the EW scale, N_3 decays into τ and an off-shell W_L via the $\nu - N$ mixing $\sim v_L / v_R$ with a typical decay

length in the lab frame

$$\left(\frac{3m_{N_3}^5}{512\pi^3 v_L^2 v_R^2}\frac{m_{N_3}}{m_{\tau'}/3}\right)^{-1} \simeq 1 \text{ mm} \left(\frac{10 \text{ GeV}}{m_{N_3}}\right)^6 \left(\frac{m_{\tau'}}{200\text{GeV}}\right)^3. \qquad (4.3)$$

For a range of m_{N_3}, the decay length is $O(1-10^3)$ mm and N_3 can be observed as a displaced vertex. However, since N_3 is highly boosted, the decay products of it are collimated and the efficiency of the reconstruction of the displaced vertex may be degraded. The estimation of the bound on $m_{\tau'}$ for this case is beyond the scope of this paper. For sufficiently small m_{N_3}, the typical decay length exceeds $O(1)$ m and N is observed as missing energy. The signal is the same as that in the previous paragraph. For m_{N_3} above the EW scale, N_3 promptly decays into $\tau + W$ or $\nu + Z/h$. See section 4.3 for the comment on the search for singlet leptons.

If N_3 is heavier than τ', τ' decays into an off-shell N_3 via W_R exchange, or into an SM fermion and a boson via the Dirac mass term $M_3 E_3 \bar{E}_3$. We first discuss the former decay mode. The off-shell W_R at least decays into ud and sc. The decay into tb is possible, but this channel is suppressed unless the Dirac mass term for the third generation up quark, M_{33}^u, is comparable to v_R so that the SM right-handed top contains a significant fraction of $SU(2)_R$ doublet. If $N_{1,2}$ are lighter than τ', decay into eN_1 and μN_2 is possible, and $N_{1,2}$ decays into SM particles as in the previous paragraph. The off-shell N_3 decays into either ν via v_L insertion, or into $\nu + Z/h$ or $\tau + W_L$, with $Z/h/W_L$ dominantly decaying into jets or leptons. For $m_{\tau'} < \text{TeV}$, the former dominates and the decay length of τ' is given by

$$\left(\frac{1}{1536\pi^3}\frac{m_{\tau'}^5 v_L^2}{v_R^6}N_f\right)^{-1} \simeq 8 \text{ mm} \times \frac{m_{\tau'}}{200 \text{ GeV}}\frac{6}{N_f}, \qquad (4.4)$$

where N_f is the number of final states. For example, if only ud and sc are available, $N_f = 6$. The decay length of τ' is above mm so τ' can be observed as di-jets from a displaced vertex. The SM neutrino from the off-shell N leads to missing energy. The most recent LHC search for displaced vertices provides upper limit for the production cross section [110] as a function of a decay length above 1 mm. Comparing it with the production cross section of hyper-charged fermions [106, 107], we obtain a bound $m_{\tau'} > 1$ TeV.

On the other hand, M_3 induces the decay of τ' into $\tau + Z/h$ or $\nu + W$, and the decay length is

$$\left(\frac{1}{4\pi}\frac{y_\tau^2 M_3^2}{m_{\tau'}}\right)^{-1} \simeq 0.1 \text{ mm} \left(\frac{3 \text{ MeV}}{M_3}\right)^2 \frac{m_{\tau'}}{200 \text{ GeV}}. \qquad (4.5)$$

For M_3 that saturates the upper bound in eq. (3.8), the decay rate is larger than that given by the W_R exchange discussed above and the decay length is below 1 mm; the decay is prompt and only the LEP bound $m_{\tau'} > 100 \text{ GeV}$ is applicable. For M_3 below the MeV scale, the decay length can be long enough that τ' can be observed as a displaced vertex, for which $m_{\tau'} > 1 \text{ TeV}$ is required.

4.3 New heavy neutral lepton

In the neutrino mass model in section 2.4.3, right-handed neutrinos mix with standard model neutrinos with the square of the angle

$$\theta_{\nu N}^2 \simeq \left(\frac{v_L}{v_R}\right)^2 = 3.3 \times 10^{-5} \left(\frac{30 \text{ TeV}}{v_R}\right)^2. \tag{4.6}$$

If the masses of them are below $100 \,\text{GeV}$, right-handed neutrinos are subject to constraints from direct searches. See [111] for the overview of constraints and prospects. This is complementary to the search for a new charged lepton, whose prospects become worse if the right-handed tau neutrino N_3 is lighter than $m_{\tau'}$. Note that N_3 is also produced from the decay of hyper-charged τ'; this may help the search for right-handed neutrinos.

4.4 New scalar particle

In section 3.2.2, we introduced a model with two singlet scalar particles, S_L and S_R, and discussed the current experimental limit. While S_R is difficult to probe, S_L can be probed via exotic decay of the SM Higgs at future colliders. In figure 2, we show the future prospects of HL-LHC and Higgs factory derived in ref. [94]. The majority of the parameter region can be probed by Higgs factories.

4.5 Electric dipole moment

The CP violation to generate baryon asymmetry in general induces electric dipole moments (EDMs) of SM fermions. In the local baryogenesis model in eq. (3.20), this is dominated by the correction from the parity partner of the operator $\propto |H_L^2|W_L\tilde{W}_L$. The correction is logarithmically enhanced by the renormalization group effect and is given by [112]

$$\frac{d_e}{e} \simeq 1 \times 10^{-30} \text{cm} \left(\frac{20 \text{ TeV}}{M}\right)^2 \frac{\ln(M^2/m_h^2)}{8}$$
$$\simeq 1 \times 10^{-30} \text{cm} \left(\frac{Y_B}{8.9 \times 10^{-11}}\right) \left(\frac{20 \text{ TeV}}{v_R}\right)^2 \left(\frac{v_R}{1.7 T_n}\right)^2 \frac{\ln(M^2/m_h^2)}{8}. \tag{4.7}$$

The current bound $d_e/e < 1.1 \times 10^{-29}$ cm [113] is satisfied for v_R above the collider bound from W_R search. Near-future detection of the electron EDM means $v_R = O(10) \,\text{TeV}$, and τ' and/or $\text{SU}(2)_R$ gauge bosons are predicted to be within the reach of near future collider experiments.

The EDM in the extra scalar model induced by the operator in eq. (3.23) is [31]

$$\frac{d_e}{e} \simeq 1 \times 10^{-31} \text{cm} \left(\frac{20 \text{ TeV}}{v_R}\right) \left(\frac{40 v_R}{M}\right) \left(\frac{\mu_S}{10 \text{ GeV}}\right)$$
$$\simeq 1 \times 10^{-31} \text{cm} \left(\frac{Y_B}{8.7 \times 10^{-11}}\right) \left(\frac{20 \text{ TeV}}{v_R}\right)^2 \left(\frac{0.2 v_R}{T_n}\right)^2 \left(\frac{\mu_S}{10 \text{ GeV}}\right)^2, \tag{4.8}$$

where we use eq. (3.24) in the second equality. The viable parameter region with $\mu_S \sim 10 \,\text{GeV}$ can be probed by future electron EDM measurements [114] if $v_R = O(10) \,\text{TeV}$.

In the model with right-handed neutrino dark matter, with the dilution in eq. (2.10), the required M becomes smaller and the prediction on the EDM becomes larger,

$$\frac{d_e}{e} \simeq 1 \times 10^{-30} \text{ cm} \left(\frac{\mu_S}{10 \text{ GeV}}\right)^2 \left(\frac{\sum_i m_{\nu_i}}{60 \text{ meV}}\right) \left(\frac{80}{g_s(T_D)}\right) \left(\frac{Y_B}{8.7 \times 10^{-11}}\right) \left(\frac{0.2 v_R}{T_n}\right)^2. \quad (4.9)$$

Interestingly, the prediction is independent of v_R and is within the reach of near-future measurements.

4.6 Gravitational waves

In order for the gravitational waves (GWs) produced by the $SU(2)_R$ phase transition to be observable, a very strong phase transition is required. A marginally SFOPT with $\langle H_R \rangle \sim T$ at the nucleation temperature is not enough, and high-temperature expansion is not justified for the analysis of very SFOPT. We thus use the full form of the 4d effective potential in appendix A to numerically compute the gravitational wave signal. The numerical computation shows that the GW signals are suppressed in the models using the running quartic coupling or extra light singlet scalars discussed in the previous sections. Here we make the following simple arguments instead of showing a detailed computation.

- For the minimal setup using the running quartic coupling, the SFOPT is achieved only for $v_R \simeq 2 \times 10^8$ GeV. Such a high v_R will make the GW-signal peak at a very high frequency, which is beyond the sensitivity of future observations.

- For the running of the quartic coupling assisted by extra leptons, the SFOPT can be achieved either by a relatively higher v_R or a smaller v_R but with a large Yukawa coupling with the extra lepton to speed up the running. For the former case, the typical frequency of GWs is too high. For the latter, the large Yukawa coupling itself also suppresses the strength of the phase transition and makes it only marginally SFOPT or even cannot achieve a SFOPT. The resultant GW signal is weak and cannot be detected.

- For the model with a light singlet scalar, the scalar is very light compared with the h_R field. This leads to a huge kinetic energy of S_R during the $SU(2)_R$ phase transition. Such a huge kinetic energy makes the duration of the phase transition short (i.e., a large β/H parameter,) and thus suppresses the GW signal [31]. Details can be found in appendix B.

In other models to realize a SFOPT, the GW signal may be observable. In such a model, the GW signal will be correlated with v_R, and hence with the new gauge boson and fermion masses and the EDM.

5 Summary and discussion

The parity solution to the strong CP problem introduces the $SU(2)_R$ gauge symmetry. In this paper, we proposed a model of baryogenesis from a first-order $SU(2)_R$ phase transition.

The key ingredient of the model is how to obtain a non-zero $B - L$ asymmetry of the SM particles. Although the $\mathrm{SU}(2)_R$ sphaleron process does not produce a non-zero charge of the naive $B - L$ symmetry with $\bar{q}(-1/3)$ and $\bar{\ell}(+1)$, the washout by the $\mathrm{SU}(2)_L$ sphaleron process is avoided if some of the asymmetry of $\mathrm{SU}(2)_R$-charged particles is (temporarily) not transferred into that of $\mathrm{SU}(2)_L$-charged particles. This is indeed possible in the model with the minimal Higgs content H_L and H_R, where the strong CP problem is solved without introducing extra symmetries. The scheme predicts a new hyper-charged fermion whose mass is correlated with the $\mathrm{SU}(2)_R$ symmetry-breaking scale v_R.

First-order $\mathrm{SU}(2)_R$ phase transition can be realized by the coupling of Higgses to other fields, as in electroweak baryogenesis. We studied two models that do not introduce extra hierarchy problems beyond that of H_R and H_L. We considered the running of the quartic coupling. If the running of the SM Higgs coupling is the SM one, $v_R > 10^8 \, \mathrm{GeV}$ is required. With Yukawa couplings to extra fermions, v_R can be much lower. We also considered a coupling of the Higgses to singlet scalar fields. v_R can be as low as the experimental lower bound from W_R search. The scalar mass is predicted to be around $10 \, \mathrm{GeV}$ and the scalar can be probed by future colliders via its mixing with the SM Higgs.

CP violation may be introduced in various ways. We applied the idea of local electroweak baryogenesis to $\mathrm{SU}(2)_R$ phase transition and studied the dimension-6 coupling of the $\mathrm{SU}(2)_R$ gauge field with H_R and the dimension-5 coupling with a singlet scalar. The higher dimensional operators generate a non-zero electron EDM that is observable in near future experiments if $v_R = O(10) \, \mathrm{TeV}$. It will be interesting to investigate other realizations of CP violation and the associated predictions on EDMs.

An obvious drawback of the model in comparison with the electroweak baryogenesis is that we generically cannot predict the scale of new physics. Indeed, the model works even if $v_R \gg 100 \, \mathrm{TeV}$, for which observable signals of the model in near future experiments are not guaranteed. However, the model still has several correlated observable signals if v_R is small enough and hence maintains predictability in a loose sense. Also, in the model with right-handed neutrino dark matter, v_R is bounded from above and the mass of a new hyper-charged fermion is predicted to be below $1 \, \mathrm{TeV}$. It will be worth considering other models with dark matter candidates and making predictions on the energy scale of parity-symmetric models.

Acknowledgments

A Uncertainties in V_{eff} computation: the Standard Model with light Higgs and top

The computation of the thermal effective potential involve uncertainties, which may introduce corresponding uncertainties in the prediction on the boundary of SFOPT, i.e., $\phi_c/T_c = 1$ [84–87]. In this appendix, we summarize different computation methods and compare their

results. Since all the SFOPT approaches mentioned in this paper are intrinsically the same as the Standard Model with a light Higgs, to make the comparison with the literature easier, we parameterize the gauge and top Yukawa couplings by the masses of particles with the symmetry breaking scale at the vacuum being the electroweak scale, i.e., 173 GeV. As is found in [81], the phase transition strength is very sensitive to the top Yukawa coupling. To analyse the $\mathrm{SU}(2)_R$ phase transition that occurs at a much higher temperature than the electroweak scale, where the top Yukawa is smaller, we choose two much smaller top Yukawa couplings that correspond to $m_t = 120$ and $90\,\mathrm{GeV}$, and slightly smaller electroweak gauge coupling constant that corresponds to $m_W = 73\,\mathrm{GeV}$, $m_Z = 83\,\mathrm{GeV}$.

At 1-loop level, a traditional computation gives the effective potential (for early papers and good reviews, see [81, 82, 84, 89, 90, 115–121])

$$V(h, T) = V_{T=0} + V_{\mathrm{FT}}, \tag{A.1}$$

where

$$V_{T=0} = -\frac{1}{2}\mu_h^2 h^2 + \frac{1}{4}\lambda h^4 + 4Bv^2 h^2 - \frac{3}{2}Bh^4 + Bh^4 \ln\left(\frac{h^2}{2v^2}\right),$$

$$B = \frac{1}{256\pi^2 v^4}\left(2m_W^4 + m_Z^4 - 4m_t^4\right),$$

$$V_{\mathrm{FT}} = \frac{T^4}{2\pi}\left(4J_B\left(\frac{m_W}{T}\right) + 2J_B\left(\frac{m_Z}{T}\right) - 12J_F\left(\frac{m_t}{T}\right)\right)$$

$$J_{B,F}(r^2) = \int_0^\infty dx x^2 \log\left(1 \mp \exp\left(-\sqrt{x^2 + r^2}\right)\right). \tag{A.2}$$

Here we use the on-shell renormalization scheme. To deal with the infrared divergence of the zero-mode of bosonic degree of freedom, proper resummation is needed. The resummation, however, is still controversial, and different resummation method causes uncertainties. A commonly used method is to add a ring-diagram contribution V_{ring} to eq. (A.2) (the Arnold-Espinosa resummation), i.e.,

$$V(h, T) = V_{T=0} + V_{\mathrm{FT}} + V_{\mathrm{ring}},$$

$$V_{\mathrm{ring}} = -\frac{T}{12\pi}\left(2(m_W(h, T)^{3/2} - m_W(h)^{3/2}) + (m_Z(h, T)^{3/2} - m_Z(h)^{3/2}) + m_B(h, T)^{3/2}\right), \tag{A.3}$$

where the temperature-dependent masses are the thermal masses and can be found in [122].

Around the boundary of SFOPT, we have $T > m(h)$ for all the degrees of freedom and we may use the high-temperature expansion

$$V = D(T^2 - T_0^2)h^2 - ETh^3 + \frac{1}{4}\lambda(T)h^4, \tag{A.4}$$

where

$$D = \frac{1}{16v^2}\left(2m_W^2 + m_Z^2 + 2m_t^2\right), \quad E = \frac{2}{3}\frac{1}{8\sqrt{2}\pi v^3}\left(2m_W^3 + m_Z^3\right), \quad T_0^2 = \frac{1}{2D}(\mu_h^2 - 4Bv^2),$$

$$\lambda(T) = \lambda - \frac{3}{64\pi^2 v^4}\left(2m_W^4 \ln\frac{m_W^2}{a_B T^2} + m_Z^4 \ln\frac{m_Z^2}{a_B T^2} - 4m_t^4 \ln\frac{m_t^2}{a_F T^2}\right). \tag{A.5}$$
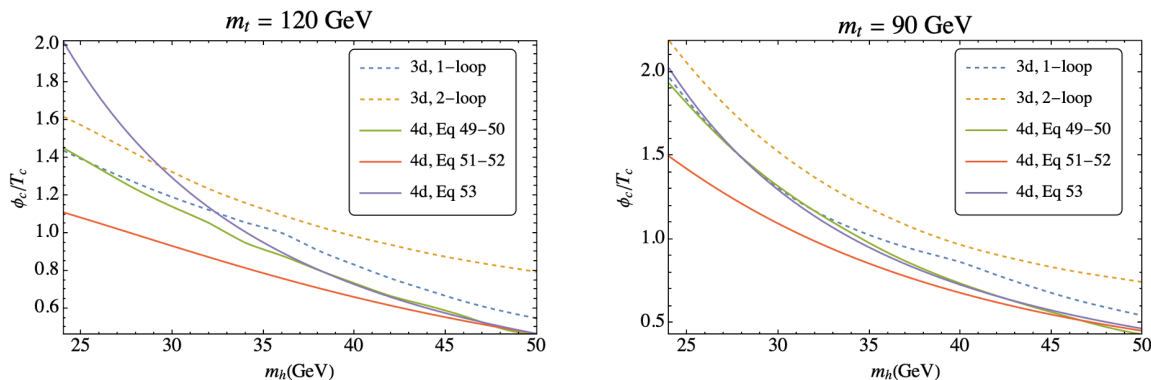
Figure 3. The phase transition strength ϕ_c/T_c under different computation methods. Dashed lines are computed in the 3d effective theory, while the solid lines are performed in the 4d theory. The 4d theories are computed under the full form (eq. (A.2)–(A.3)), or high-temperature expansion with (eq. (A.4)–(A.5)) or without (eq. (A.6)) the leading log terms.

Here $\log a_B = 2\log 4\pi - 2\gamma_E$ and $\log a_F = 2\log \pi - 2\gamma_E$, with γ_E the Euler-gamma. Here we add a factor of $2/3$ in the E term to screen out the longitudinal instead of adding the ring-diagram term. We can further simplify the expression by neglecting the log terms, which leads to the most simplified expression

$$V = D(T^2 - T_0^2)h^2 - ETh^3 + \frac{1}{4}\lambda h^4,$$
$$D = \frac{1}{16v^2}\left(2m_W^2 + m_Z^2 + 2m_t^2\right), \ E = \frac{2}{3}\frac{1}{8\sqrt{2}\pi v^3}\left(2m_W^3 + m_Z^3\right), \ T_0^2 = \frac{1}{2D}\mu_h^2. \quad (A.6)$$

The phase transition strength ϕ_c/T_c can be simply expressed as $2E/\lambda$ under this expression, and we can see that a smaller quartic coupling λ leads to large phase transition strength. Even for the cases where the high-temperature expansion is not a good approximation, this still provides a useful intuition.

The main problem of eq. (A.6), however, is its complete ignorance of the zero-temperature correction. From eq. (A.5) where such an effect is included, we can see that the λ receives a positive contribution from the top Yukawa coupling, i.e. m_t, which suppresses the phase transition strength. Such a result is confirmed by numerical computation from the full form. The suppression of the phase transition strength by the top Yukawa is relieved at a high v_R, since the top Yukawa coupling is much smaller than that at the EW scale due to running.

On the other hand, the state-of-the-art method to perform the thermal resummation is to integrate out the zero mode of the bosonic degrees of freedom and work in an effective dimension-3 theory, so-called the dimensional reduction [123–127]. This computation method is theoretically more reliable while also being more complicated. With the help of the recently published `Mathematica` package `DRalgo` [128], we compute the thermal potential up to 2-loop level. In figure (3), we show the comparison of different computation methods. One can see that the agreement between different approximation methods gets better for smaller m_t. Since scanning over the parameter space using the dimensional

reduction with 2-loop correction is complicated, we use the approximation in eq. (A.6) to derive the boundary of the SFOPT in the main text because of its simplicity while being in reasonable agreement with the state-of-the-art 2-loop computation result.

B Analysis of the light scalar model

In section 3.2.2, we proposed a model with a naturally light scalar to enhance the phase transition. In this appendix, we discuss some important features of this model, including the fine-tuning of the scalar mass and the origin of large β/H, which is relevant to the discussion of the gravitational-wave signals. As in the previous section, we analyze the SM with a lighter top quark mass $m_t = 120$ GeV. The Higgs boson and gauge boson masses are chosen to be the Standard Model values at EW scale.

The tree-level potential can be written as [30, 31]

$$V_0 = -\frac{1}{2}\mu_h^2 h^2 + \frac{1}{4}\lambda h^4 + \frac{1}{2}\mu_S^2 S^2 - \frac{1}{2}AS(h^2 - 2v^2), \tag{B.1}$$

where h is the SM Higgs field, $v \simeq 174$ GeV is the electroweak vev, and S is an extra scalar. An approximate shift symmetry $S \to S + \delta S$, softly broken by the mass term and the trilinear coupling A, avoids an extra hierarchy problem; the lightness of S is natural [31]. Higher order terms of S is forbidden by the shift symmetry.

For a given field value of h, we may minimize the potential with respect to S,

$$\langle S \rangle = \frac{A}{2\mu_S^2}h^2 + \text{const},$$
$$V_0 = -\frac{1}{2}\mu_h^2 h^2 + \frac{1}{4}\left(\lambda - \frac{A^2}{2\mu_S^2}\right)h^4. \tag{B.2}$$

One can see that along this path, the effective Higgs quartic coupling λ is corrected to be $\lambda_{\text{eff}} = \lambda - A^2/2\mu_S^2 < \lambda$, which can induce a strong first-order phase transition.

The physical mass eigenstates are

$$m_+^2 \equiv m_h^2 \simeq 4\lambda v^2 \left(1 + \frac{A^2}{8\lambda^2 v^2}\right),$$
$$m_-^2 \equiv m_S^2 \simeq \mu_S^2 - \frac{A^2}{2\lambda}. \tag{B.3}$$

The full tree-level relationship between parameters can be found in ref. [31]. The fine-tuning of this model can be defined as

$$\text{fine-tuning} \equiv \frac{\lambda - A^2/2\mu_S^2}{\lambda} = \frac{m_S^2}{\mu_S^2}. \tag{B.4}$$

From eq. (B.2), one can see that the field shift of S is very large for a light μ_S during the phase transition, if the phase transition path is indeed along that path. Numerical
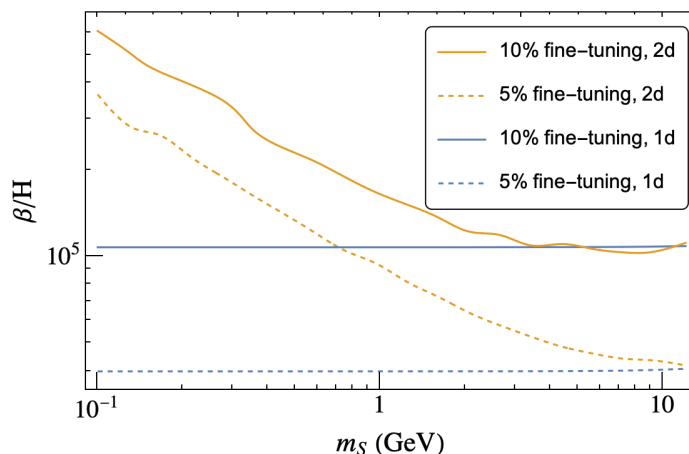
Figure 4. β/H as a function of m_S for fixed fine-tuning 5% and 10%. 1d: the bounce action is obtained along the path in eq. (B.2) with the kinetic term of S neglected. 2d: full two-field dynamics is included.

solution to the bounce equation shows that it is indeed the case. The gradient term of the S field, K_S, is much larger compared to that of the Higgs field, K_h;

$$\frac{K_S}{K_h} \equiv \left(\frac{dS}{dr}\right)^2 / \left(\frac{dh}{dr}\right)^2 = \frac{A^2}{\mu_S^2}\frac{h^2}{\mu_S^2} = 2\lambda\left(1 - \text{fine-tuning}\right)\frac{h^2}{\mu_S^2} \simeq 2\lambda\left(1 - \text{fine-tuning}\right)\frac{v^2}{\mu_S^2}, \tag{B.5}$$

where r is the space variable along the bubble profile, $S(r)$ and $h(r)$ are the singlet and Higgs field along the bubble profile, respectively. The kinetic energy E_{k_i} is defined as the integral of $r^2 K_i/2$ along the bubble profile. From eq. (B.5), one can see that a large v/μ_S ratio leads to large kinetic energy of S. As the temperature cools down, this large, positive contribution to the 3d Euclidean action S_3 is canceled by the negative contribution from the potential energy so that $S_3/T \simeq 140$ is finally reached for bubbles to efficiently nucleate. However, the cancellation does not occur for the derivative of S_3/T, causing a large $\beta/H \equiv Td(S_3/T)/dT$ at the nucleation temperature.

In figure 2, we show β/H as a function of m_S for fixed fine-tuning 5% and 10%. For the orange lines labelled "2d", we obtain the bounce action with the full two-field dynamics of h and S. One can easily see that β/H increases for smaller μ_S. In the parity-symmetric model, the relevant ratio v_R/μ_S is order-of-magnitude larger than v/μ_S in the electroweak case in the allowed parameter space in figure 2, so we expect that the β/H quantity is even larger than that in figure 4, which suppresses the gravitational wave signal. For a comparison, we also obtain the bounce action along the path in the first line of eq. (B.2) ignoring the kinetic term of S, which corresponds to the one-field dynamics of h with the potential in the second line of eq. (B.2). The resultant β/H is shown by blue lines in figure 4. For large m_S, the result is in good agreement with the result of the full two-field computation, since the field excursion of S is small and the kinetic term of S is negligible. For small m_S, the kinetic term of S is not negligible and one should solve the full two-field dynamics.

References

[1] J.S. Bell and R. Jackiw, *A PCAC puzzle: $\pi^0 \to \gamma\gamma$ in the σ model*, [*Nuovo Cim. A* **60** (1969) 47](https://doi.org/) [[INSPIRE](https://inspirehep.net/)].

[2] S.L. Adler, *Axial vector vertex in spinor electrodynamics*, [*Phys. Rev.* **177** (1969) 2426](https://doi.org/) [[INSPIRE](https://inspirehep.net/)].

[3] G. 't Hooft, *Symmetry Breaking Through Bell-Jackiw Anomalies*, [*Phys. Rev. Lett.* **37** (1976) 8](https://doi.org/) [[INSPIRE](https://inspirehep.net/)].

[4] G. 't Hooft, *Computation of the Quantum Effects Due to a Four-Dimensional Pseudoparticle*, [*Phys. Rev. D* **14** (1976) 3432](https://doi.org/) [*Erratum ibid.* **18** (1978) 2199] [[INSPIRE](https://inspirehep.net/)].

[5] C. Abel et al., *Measurement of the Permanent Electric Dipole Moment of the Neutron*, [*Phys. Rev. Lett.* **124** (2020) 081803](https://doi.org/) [[arXiv:2001.11966](https://arxiv.org/abs/2001.11966)] [[INSPIRE](https://inspirehep.net/)].

[6] M.A.B. Beg and H.-S. Tsao, *Strong P, T Noninvariances in a Superweak Theory*, [*Phys. Rev. Lett.* **41** (1978) 278](https://doi.org/) [[INSPIRE](https://inspirehep.net/)].

[7] R.N. Mohapatra and G. Senjanovic, *Natural Suppression of Strong p and t Noninvariance*, [*Phys. Lett. B* **79** (1978) 283](https://doi.org/) [[INSPIRE](https://inspirehep.net/)].

[8] K.S. Babu and R.N. Mohapatra, *CP Violation in Seesaw Models of Quark Masses*, [*Phys. Rev. Lett.* **62** (1989) 1079](https://doi.org/) [[INSPIRE](https://inspirehep.net/)].

[9] K.S. Babu and R.N. Mohapatra, *A Solution to the Strong CP Problem Without an Axion*, [*Phys. Rev. D* **41** (1990) 1286](https://doi.org/) [[INSPIRE](https://inspirehep.net/)].

[10] R. Kuchimanchi, *Solution to the strong CP problem: Supersymmetry with parity*, [*Phys. Rev. Lett.* **76** (1996) 3486](https://doi.org/) [[hep-ph/9511376](https://arxiv.org/abs/hep-ph/9511376)] [[INSPIRE](https://inspirehep.net/)].

[11] R.N. Mohapatra and A. Rasin, *Simple supersymmetric solution to the strong CP problem*, [*Phys. Rev. Lett.* **76** (1996) 3490](https://doi.org/) [[hep-ph/9511391](https://arxiv.org/abs/hep-ph/9511391)] [[INSPIRE](https://inspirehep.net/)].

[12] L.J. Hall and K. Harigaya, *Implications of Higgs Discovery for the Strong CP Problem and Unification*, [*JHEP* **10** (2018) 130](https://doi.org/) [[arXiv:1803.08119](https://arxiv.org/abs/1803.08119)] [[INSPIRE](https://inspirehep.net/)].

[13] J. de Vries, P. Draper and H.H. Patel, *Do Minimal Parity Solutions to the Strong CP Problem Work?*, [arXiv:2109.01630](https://arxiv.org/abs/2109.01630) [[INSPIRE](https://inspirehep.net/)].

[14] V.A. Kuzmin, V.A. Rubakov and M.E. Shaposhnikov, *On the Anomalous Electroweak Baryon Number Nonconservation in the Early Universe*, [*Phys. Lett. B* **155** (1985) 36](https://doi.org/) [[INSPIRE](https://inspirehep.net/)].

[15] A.I. Bochkarev and M.E. Shaposhnikov, *Electroweak Production of Baryon Asymmetry and Upper Bounds on the Higgs and Top Masses*, [*Mod. Phys. Lett. A* **2** (1987) 417](https://doi.org/) [[INSPIRE](https://inspirehep.net/)].

[16] G.W. Anderson and L.J. Hall, *The Electroweak phase transition and baryogenesis*, [*Phys. Rev. D* **45** (1992) 2685](https://doi.org/) [[INSPIRE](https://inspirehep.net/)].

[17] J.R. Espinosa and M. Quiros, *The Electroweak phase transition with a singlet*, [*Phys. Lett. B* **305** (1993) 98](https://doi.org/) [[hep-ph/9301285](https://arxiv.org/abs/hep-ph/9301285)] [[INSPIRE](https://inspirehep.net/)].

[18] J.R. Espinosa, M. Quiros and F. Zwirner, *On the electroweak phase transition in the minimal supersymmetric Standard Model*, [*Phys. Lett. B* **307** (1993) 106](https://doi.org/) [[hep-ph/9303317](https://arxiv.org/abs/hep-ph/9303317)] [[INSPIRE](https://inspirehep.net/)].

[19] D. Bödeker, P. John, M. Laine and M.G. Schmidt, *The Two loop MSSM finite temperature effective potential with stop condensation*, *Nucl. Phys. B* **497** (1997) 387 [`hep-ph/9612364`] [InSPIRE].

[20] M. Carena, M. Quiros and C.E.M. Wagner, *Opening the window for electroweak baryogenesis*, *Phys. Lett. B* **380** (1996) 81 [`hep-ph/9603420`] [InSPIRE].

[21] J.R. Espinosa, *Dominant two loop corrections to the MSSM finite temperature effective potential*, *Nucl. Phys. B* **475** (1996) 273 [`hep-ph/9604320`] [InSPIRE].

[22] M. Carena, M. Quiros and C.E.M. Wagner, *Electroweak baryogenesis and Higgs and stop searches at LEP and the Tevatron*, *Nucl. Phys. B* **524** (1998) 3 [`hep-ph/9710401`] [InSPIRE].

[23] J.M. Cline and G.D. Moore, *Supersymmetric electroweak phase transition: Baryogenesis versus experimental constraints*, *Phys. Rev. Lett.* **81** (1998) 3315 [`hep-ph/9806354`] [InSPIRE].

[24] M. Pietroni, *The Electroweak phase transition in a nonminimal supersymmetric model*, *Nucl. Phys. B* **402** (1993) 27 [`hep-ph/9207227`] [InSPIRE].

[25] J. Choi and R.R. Volkas, *Real Higgs singlet and the electroweak phase transition in the Standard Model*, *Phys. Lett. B* **317** (1993) 385 [`hep-ph/9308234`] [InSPIRE].

[26] N. Turok and J. Zadrozny, *Phase transitions in the two doublet model*, *Nucl. Phys. B* **369** (1992) 729 [InSPIRE].

[27] J.M. Cline, K. Kainulainen and A.P. Vischer, *Dynamics of two Higgs doublet CP violation and baryogenesis at the electroweak phase transition*, *Phys. Rev. D* **54** (1996) 2451 [`hep-ph/9506284`] [InSPIRE].

[28] J.M. Cline and P.-A. Lemieux, *Electroweak phase transition in two Higgs doublet models*, *Phys. Rev. D* **55** (1997) 3873 [`hep-ph/9609240`] [InSPIRE].

[29] V. Barger et al., *Complex Singlet Extension of the Standard Model*, *Phys. Rev. D* **79** (2009) 015018 [`arXiv:0811.0393`] [InSPIRE].

[30] S. Das, P.J. Fox, A. Kumar and N. Weiner, *The Dark Side of the Electroweak Phase Transition*, *JHEP* **11** (2010) 108 [`arXiv:0910.1262`] [InSPIRE].

[31] K. Harigaya and I.R. Wang, *First-Order Electroweak Phase Transition and Baryogenesis from a Naturally Light Singlet Scalar*, [`arXiv:2207.02867`] [InSPIRE].

[32] M. Dine, P. Huet, R.L. Singleton Jr. and L. Susskind, *Creating the baryon asymmetry at the electroweak phase transition*, *Phys. Lett. B* **257** (1991) 351 [InSPIRE].

[33] V. Brdar, L. Graf, A.J. Helmboldt and X.-J. Xu, *Gravitational Waves as a Probe of Left-Right Symmetry Breaking*, *JCAP* **12** (2019) 027 [`arXiv:1909.02018`] [InSPIRE].

[34] K. Fujikura, K. Harigaya, Y. Nakai and I.R. Wang, *Electroweak-like baryogenesis with new chiral matter*, *JHEP* **07** (2021) 224 [*Erratum ibid.* **12** (2021) 192] [`arXiv:2103.05005`] [InSPIRE].

[35] J. Shu, T.M.P. Tait and C.E.M. Wagner, *Baryogenesis from an Earlier Phase Transition*, *Phys. Rev. D* **75** (2007) 063510 [`hep-ph/0610375`] [InSPIRE].

[36] J. Shelton and K.M. Zurek, *Darkogenesis: A baryon asymmetry from the dark matter sector*, *Phys. Rev. D* **82** (2010) 123512 [`arXiv:1008.1997`] [InSPIRE].

[37] H. Davoudiasl, P.P. Giardino and C. Zhang, *Higgs-like boson at 750 GeV and genesis of baryons*, *Phys. Rev. D* **94** (2016) 015006 [`arXiv:1605.00037`] [InSPIRE].

[38] B. Fornal, Y. Shirman, T.M.P. Tait and J.R. West, *Asymmetric dark matter and baryogenesis from* SU(2)$_\ell$, *Phys. Rev. D* **96** (2017) 035001 [arXiv:1703.00199] [INSPIRE].

[39] E. Hall et al., *Baryogenesis From a Dark First-Order Phase Transition*, *JHEP* **04** (2020) 042 [arXiv:1910.08068] [INSPIRE].

[40] V. Agrawal, S.M. Barr, J.F. Donoghue and D. Seckel, *Viable range of the mass scale of the standard model*, *Phys. Rev. D* **57** (1998) 5480 [hep-ph/9707380] [INSPIRE].

[41] L.J. Hall, D. Pinner and J.T. Ruderman, *The Weak Scale from BBN*, *JHEP* **12** (2014) 134 [arXiv:1409.0551] [INSPIRE].

[42] G. D'Amico, A. Strumia, A. Urbano and W. Xue, *Direct anthropic bound on the weak scale from supernovæ explosions*, *Phys. Rev. D* **100** (2019) 083013 [arXiv:1906.00986] [INSPIRE].

[43] R. Kawasaki, T. Morozumi and H. Umeeda, *Quark sector CP violation of the universal seesaw model*, *Phys. Rev. D* **88** (2013) 033019 [arXiv:1306.5080] [INSPIRE].

[44] K.S. Babu, B. Dutta and R.N. Mohapatra, *A theory of* $R(D^*, D)$ *anomaly with right-handed currents*, *JHEP* **01** (2019) 168 [arXiv:1811.04496] [INSPIRE].

[45] N. Craig, I. Garcia Garcia, G. Koszegi and A. McCune, *P not PQ*, *JHEP* **09** (2021) 130 [arXiv:2012.13416] [INSPIRE].

[46] ATLAS collaboration, *Search for pair production of a new heavy quark that decays into a W boson and a light quark in pp collisions at* $\sqrt{s} = 8$ *TeV with the ATLAS detector*, *Phys. Rev. D* **92** (2015) 112007 [arXiv:1509.04261] [INSPIRE].

[47] CMS collaboration, *Search for vectorlike light-flavor quark partners in proton-proton collisions at* $\sqrt{s} = 8$ *TeV*, *Phys. Rev. D* **97** (2018) 072008 [arXiv:1708.02510] [INSPIRE].

[48] ATLAS collaboration, *Combination of the searches for pair-produced vector-like partners of the third-generation quarks at* $\sqrt{s} = 13$ *TeV with the ATLAS detector*, *Phys. Rev. Lett.* **121** (2018) 211801 [arXiv:1808.02343] [INSPIRE].

[49] CMS collaboration, *Search for vector-like T and B quark pairs in final states with leptons at* $\sqrt{s} = 13$ *TeV*, *JHEP* **08** (2018) 177 [arXiv:1805.04758] [INSPIRE].

[50] T. Yanagida, *Horizontal gauge symmetry and masses of neutrinos*, *Conf. Proc. C* **7902131** (1979) 95 [INSPIRE].

[51] M. Gell-Mann, P. Ramond and R. Slansky, *Complex Spinors and Unified Theories*, *Conf. Proc. C* **790927** (1979) 315 [arXiv:1306.4669] [INSPIRE].

[52] P. Minkowski, $\mu \to e\gamma$ *at a Rate of One Out of* 10^9 *Muon Decays?*, *Phys. Lett. B* **67** (1977) 421 [INSPIRE].

[53] R.N. Mohapatra and G. Senjanovic, *Neutrino Mass and Spontaneous Parity Nonconservation*, *Phys. Rev. Lett.* **44** (1980) 912 [INSPIRE].

[54] M. Viel, G.D. Becker, J.S. Bolton and M.G. Haehnelt, *Warm dark matter as a solution to the small scale crisis: New constraints from high redshift Lyman-α forest data*, *Phys. Rev. D* **88** (2013) 043502 [arXiv:1306.2314] [INSPIRE].

[55] V. Iršič et al., *New Constraints on the free-streaming of warm dark matter from intermediate and small scale Lyman-α forest data*, *Phys. Rev. D* **96** (2017) 023522 [arXiv:1702.01764] [INSPIRE].

[56] N. Palanque-Delabrouille et al., *Hints, neutrino bounds and WDM constraints from SDSS DR14 Lyman-α and Planck full-survey data*, *JCAP* **04** (2020) 038 [arXiv:1911.09073] [ɪɴSPIRE].

[57] A. Garzilli, A. Magalich, O. Ruchayskiy and A. Boyarsky, *How to constrain warm dark matter with the Lyman-α forest*, *Mon. Not. Roy. Astron. Soc.* **502** (2021) 2356 [arXiv:1912.09397] [ɪɴSPIRE].

[58] F. Bezrukov, H. Hettmansperger and M. Lindner, *keV sterile neutrino Dark Matter in gauge extensions of the Standard Model*, *Phys. Rev. D* **81** (2010) 085032 [arXiv:0912.4415] [ɪɴSPIRE].

[59] A. Greljo, D.J. Robinson, B. Shakya and J. Zupan, $R(D^{(*)})$ *from* W' *and right-handed neutrinos*, *JHEP* **09** (2018) 169 [arXiv:1804.04642] [ɪɴSPIRE].

[60] J.A. Dror, D. Dunsky, L.J. Hall and K. Harigaya, *Sterile Neutrino Dark Matter in Left-Right Theories*, *JHEP* **07** (2020) 168 [arXiv:2004.09511] [ɪɴSPIRE].

[61] PLANCK collaboration, *Planck 2018 results. VI. Cosmological parameters*, *Astron. Astrophys.* **641** (2020) A6 [*Erratum ibid.* **652** (2021) C4] [arXiv:1807.06209] [ɪɴSPIRE].

[62] J. Carrasco-Martinez, D.I. Dunsky, L.J. Hall and K. Harigaya, *Leptogenesis in Parity Solutions to the Strong CP Problem and Standard Model Parameters*, arXiv:2307.15731 [ɪɴSPIRE].

[63] P.S.B. Dev and A. Pilaftsis, *Minimal Radiative Neutrino Mass Mechanism for Inverse Seesaw Models*, *Phys. Rev. D* **86** (2012) 113001 [arXiv:1209.4051] [ɪɴSPIRE].

[64] D. Bödeker and D. Schröder, *Equilibration of right-handed electrons*, *JCAP* **05** (2019) 010 [arXiv:1902.07220] [ɪɴSPIRE].

[65] K. Harigaya and I.R. Wang, *Axiogenesis from* SU(2)$_R$ *phase transition*, *JHEP* **10** (2021) 022 [*Erratum ibid.* **12** (2021) 193] [arXiv:2107.09679] [ɪɴSPIRE].

[66] B.A. Campbell, S. Davidson, J.R. Ellis and K.A. Olive, *On the baryon, lepton flavor and right-handed electron asymmetries of the universe*, *Phys. Lett. B* **297** (1992) 118 [hep-ph/9302221] [ɪɴSPIRE].

[67] J.M. Cline, K. Kainulainen and K.A. Olive, *On the erasure and regeneration of the primordial baryon asymmetry by sphalerons*, *Phys. Rev. Lett.* **71** (1993) 2372 [hep-ph/9304321] [ɪɴSPIRE].

[68] J.M. Cline, K. Kainulainen and K.A. Olive, *Protecting the primordial baryon asymmetry from erasure by sphalerons*, *Phys. Rev. D* **49** (1994) 6394 [hep-ph/9401208] [ɪɴSPIRE].

[69] M. Fukugita and T. Yanagida, *Resurrection of grand unified theory baryogenesis*, *Phys. Rev. Lett.* **89** (2002) 131602 [hep-ph/0203194] [ɪɴSPIRE].

[70] V. Domcke et al., *Wash-In Leptogenesis*, *Phys. Rev. Lett.* **126** (2021) 201802 [arXiv:2011.09347] [ɪɴSPIRE].

[71] J.A. Harvey and M.S. Turner, *Cosmological baryon and lepton number in the presence of electroweak fermion number violation*, *Phys. Rev. D* **42** (1990) 3344 [ɪɴSPIRE].

[72] R.T. Co and K. Harigaya, *Axiogenesis*, *Phys. Rev. Lett.* **124** (2020) 111602 [arXiv:1910.02080] [ɪɴSPIRE].

[73] S. Davidson and J.R. Ellis, *Basis independent measures of R-parity violation*, *Phys. Lett. B* **390** (1997) 210 [hep-ph/9609451] [ɪɴSPIRE].

[74] S. Davidson and J.R. Ellis, *Flavor dependent and basis independent measures of R violation*, *Phys. Rev. D* **56** (1997) 4182 [hep-ph/9702247] [INSPIRE].

[75] K. Kajantie, M. Laine, K. Rummukainen and M.E. Shaposhnikov, *The Electroweak phase transition: A Nonperturbative analysis*, *Nucl. Phys. B* **466** (1996) 189 [hep-lat/9510020] [INSPIRE].

[76] K. Kajantie, M. Laine, K. Rummukainen and M.E. Shaposhnikov, *Is there a hot electroweak phase transition at $m_H \gtrsim m_W$?*, *Phys. Rev. Lett.* **77** (1996) 2887 [hep-ph/9605288] [INSPIRE].

[77] M. Gurtler, E.-M. Ilgenfritz and A. Schiller, *Where the electroweak phase transition ends*, *Phys. Rev. D* **56** (1997) 3888 [hep-lat/9704013] [INSPIRE].

[78] K. Rummukainen et al., *The Universality class of the electroweak theory*, *Nucl. Phys. B* **532** (1998) 283 [hep-lat/9805013] [INSPIRE].

[79] F. Csikor, Z. Fodor and J. Heitger, *Endpoint of the hot electroweak phase transition*, *Phys. Rev. Lett.* **82** (1999) 21 [hep-ph/9809291] [INSPIRE].

[80] K. Jansen, *Status of the finite temperature electroweak phase transition on the lattice*, *Nucl. Phys. B Proc. Suppl.* **47** (1996) 196 [hep-lat/9509018] [INSPIRE].

[81] M. Dine et al., *Towards the theory of the electroweak phase transition*, *Phys. Rev. D* **46** (1992) 550 [hep-ph/9203203] [INSPIRE].

[82] P.B. Arnold and O. Espinosa, *The Effective potential and first order phase transitions: Beyond leading-order*, *Phys. Rev. D* **47** (1993) 3546 [*Erratum ibid.* **50** (1994) 6662] [hep-ph/9212235] [INSPIRE].

[83] J.R. Espinosa, *Tunneling without Bounce*, *Phys. Rev. D* **100** (2019) 105002 [arXiv:1908.01730] [INSPIRE].

[84] D. Croon et al., *Theoretical uncertainties for cosmological first-order phase transitions*, *JHEP* **04** (2021) 055 [arXiv:2009.10080] [INSPIRE].

[85] P.M. Schicho, T.V.I. Tenkanen and J. Österman, *Robust approach to thermal resummation: Standard Model meets a singlet*, *JHEP* **06** (2021) 130 [arXiv:2102.11145] [INSPIRE].

[86] L. Niemi, P. Schicho and T.V.I. Tenkanen, *Singlet-assisted electroweak phase transition at two loops*, *Phys. Rev. D* **103** (2021) 115035 [arXiv:2103.07467] [INSPIRE].

[87] P. Schicho, T.V.I. Tenkanen and G. White, *Combining thermal resummation and gauge invariance for electroweak phase transition*, *JHEP* **11** (2022) 047 [arXiv:2203.04284] [INSPIRE].

[88] PARTICLE DATA GROUP collaboration, *Review of Particle Physics*, *PTEP* **2022** (2022) 083C01 [INSPIRE].

[89] D.E. Morrissey and M.J. Ramsey-Musolf, *Electroweak baryogenesis*, *New J. Phys.* **14** (2012) 125003 [arXiv:1206.2942] [INSPIRE].

[90] M. Quiros, *Finite temperature field theory and phase transitions*, in the proceedings of the *ICTP Summer School in High-Energy Physics and Cosmology*, Trieste Italy, June 02–July 11 (1997), p. 187–259 [hep-ph/9901312] [INSPIRE].

[91] LEP WORKING GROUP FOR HIGGS BOSON SEARCHES et al. collaborations, *Search for the standard model Higgs boson at LEP*, *Phys. Lett. B* **565** (2003) 61 [hep-ex/0306033] [INSPIRE].

[92] L3 collaboration, *Search for neutral Higgs boson production through the process* $e^+e^- \to Z^*H^0$, *Phys. Lett. B* **385** (1996) 454 [INSPIRE].

[93] OPAL collaboration, *Decay mode independent searches for new scalar bosons with the OPAL detector at LEP*, *Eur. Phys. J. C* **27** (2003) 311 [hep-ex/0206022] [INSPIRE].

[94] M. Carena et al., *Probing the Electroweak Phase Transition with Exotic Higgs Decays*, *LHEP* **2023** (2023) 432 [arXiv:2203.08206] [INSPIRE].

[95] J. Beacham et al., *Physics Beyond Colliders at CERN: Beyond the Standard Model Working Group Report*, *J. Phys. G* **47** (2020) 010501 [arXiv:1901.09966] [INSPIRE].

[96] E. Goudzovski et al., *New physics searches at kaon and hyperon factories*, *Rept. Prog. Phys.* **86** (2023) 016201 [arXiv:2201.07805] [INSPIRE].

[97] LHCb collaboration, *Search for long-lived scalar particles in* $B^+ \to K^+\chi(\mu^+\mu^-)$ *decays*, *Phys. Rev. D* **95** (2017) 071101 [arXiv:1612.07818] [INSPIRE].

[98] LHCb collaboration, *Search for hidden-sector bosons in* $B^0 \to K^{*0}\mu^+\mu^-$ *decays*, *Phys. Rev. Lett.* **115** (2015) 161802 [arXiv:1508.04094] [INSPIRE].

[99] NA62 collaboration, *Search for* π^0 *decays to invisible particles*, *JHEP* **02** (2021) 201 [arXiv:2010.07644] [INSPIRE].

[100] NA62 collaboration, *Measurement of the very rare* $K^+ \to \pi^+\nu\overline{\nu}$ *decay*, *JHEP* **06** (2021) 093 [arXiv:2103.15389] [INSPIRE].

[101] M. Ibe, S. Kobayashi, Y. Nakayama and S. Shirai, *Cosmological constraints on dark scalar*, *JHEP* **03** (2022) 198 [arXiv:2112.11096] [INSPIRE].

[102] M. D'Onofrio, K. Rummukainen and A. Tranberg, *Sphaleron Rate in the Minimal Standard Model*, *Phys. Rev. Lett.* **113** (2014) 141602 [arXiv:1404.3565] [INSPIRE].

[103] J.B. Muñoz, C. Dvorkin and F.-Y. Cyr-Racine, *Probing the Small-Scale Matter Power Spectrum with Large-Scale* 21 *cm Data*, *Phys. Rev. D* **101** (2020) 063526 [arXiv:1911.11144] [INSPIRE].

[104] ATLAS collaboration, *Search for a heavy charged boson in events with a charged lepton and missing transverse momentum from pp collisions at* $\sqrt{s} = 13$ *TeV with the ATLAS detector*, *Phys. Rev. D* **100** (2019) 052013 [arXiv:1906.05609] [INSPIRE].

[105] ATLAS collaboration, *Prospects for searches for heavy* Z' *and* W' *bosons in fermionic final states with the ATLAS experiment at the HL-LHC*, ATL-PHYS-PUB-2018-044, CERN, Geneva (2018).

[106] N. Kumar and S.P. Martin, *Vectorlike Leptons at the Large Hadron Collider*, *Phys. Rev. D* **92** (2015) 115018 [arXiv:1510.03456] [INSPIRE].

[107] P.N. Bhattiprolu and S.P. Martin, *Prospects for vectorlike leptons at future proton-proton colliders*, *Phys. Rev. D* **100** (2019) 015033 [arXiv:1905.00498] [INSPIRE].

[108] ATLAS collaboration, *Search for electroweak production of charginos and sleptons decaying into final states with two leptons and missing transverse momentum in* $\sqrt{s} = 13$ *TeV pp collisions using the ATLAS detector*, *Eur. Phys. J. C* **80** (2020) 123 [arXiv:1908.08215] [INSPIRE].

[109] L3 collaboration, *Search for heavy neutral and charged leptons in* e^+e^- *annihilation at LEP*, *Phys. Lett. B* **517** (2001) 75 [hep-ex/0107015] [INSPIRE].

[110] CMS collaboration, *Search for long-lived particles using displaced jets in proton-proton collisions at $\sqrt{s} = 13$ TeV*, *Phys. Rev. D* **104** (2021) 012015 [`arXiv:2012.01581`] [InSPIRE].

[111] A.M. Abdullahi et al., *The present and future status of heavy neutral leptons*, *J. Phys. G* **50** (2023) 020501 [`arXiv:2203.08039`] [InSPIRE].

[112] A. Lue, K. Rajagopal and M. Trodden, *Semianalytical approaches to local electroweak baryogenesis*, *Phys. Rev. D* **56** (1997) 1250 [`hep-ph/9612282`] [InSPIRE].

[113] ACME collaboration, *Improved limit on the electric dipole moment of the electron*, *Nature* **562** (2018) 355 [InSPIRE].

[114] A.C. Vutha et al., *Search for the electric dipole moment of the electron with thorium monoxide*, *J. Phys. B* **43** (2010) 074007 [`arXiv:0908.2412`] [InSPIRE].

[115] S.R. Coleman and E.J. Weinberg, *Radiative Corrections as the Origin of Spontaneous Symmetry Breaking*, *Phys. Rev. D* **7** (1973) 1888 [InSPIRE].

[116] R. Jackiw, *Functional evaluation of the effective potential*, *Phys. Rev. D* **9** (1974) 1686 [InSPIRE].

[117] J.S. Kang, *Gauge Invariance of the Scalar-Vector Mass Ratio in the Coleman-Weinberg Model*, *Phys. Rev. D* **10** (1974) 3455 [InSPIRE].

[118] L. Dolan and R. Jackiw, *Gauge Invariant Signal for Gauge Symmetry Breaking*, *Phys. Rev. D* **9** (1974) 2904 [InSPIRE].

[119] R. Fukuda and T. Kugo, *Gauge Invariance in the Effective Action and Potential*, *Phys. Rev. D* **13** (1976) 3469 [InSPIRE].

[120] I.J.R. Aitchison and C.M. Fraser, *Gauge Invariance and the Effective Potential*, *Annals Phys.* **156** (1984) 1 [InSPIRE].

[121] W. Loinaz and R.S. Willey, *Gauge dependence of lower bounds on the Higgs mass derived from electroweak vacuum stability constraints*, *Phys. Rev. D* **56** (1997) 7416 [`hep-ph/9702321`] [InSPIRE].

[122] M.E. Carrington, *The Effective potential at finite temperature in the Standard Model*, *Phys. Rev. D* **45** (1992) 2933 [InSPIRE].

[123] P.H. Ginsparg, *First Order and Second Order Phase Transitions in Gauge Theories at Finite Temperature*, *Nucl. Phys. B* **170** (1980) 388 [InSPIRE].

[124] T. Appelquist and R.D. Pisarski, *High-Temperature Yang-Mills Theories and Three-Dimensional Quantum Chromodynamics*, *Phys. Rev. D* **23** (1981) 2305 [InSPIRE].

[125] S. Nadkarni, *Dimensional Reduction in Hot QCD*, *Phys. Rev. D* **27** (1983) 917 [InSPIRE].

[126] N.P. Landsman, *Limitations to Dimensional Reduction at High Temperature*, *Nucl. Phys. B* **322** (1989) 498 [InSPIRE].

[127] K. Kajantie, M. Laine, K. Rummukainen and M.E. Shaposhnikov, *Generic rules for high temperature dimensional reduction and their application to the standard model*, *Nucl. Phys. B* **458** (1996) 90 [`hep-ph/9508379`] [InSPIRE].

[128] A. Ekstedt, P. Schicho and T.V.I. Tenkanen, *DRalgo: A package for effective field theory approach for thermal phase transitions*, *Comput. Phys. Commun.* **288** (2023) 108725 [`arXiv:2205.08815`] [InSPIRE].